

**A Conceptual Model for Eight-Hour Ozone
Exceedances in Houston, Texas
Part I: Background Ozone Levels in Eastern Texas**

John W. Nielsen-Gammon, James Tobin, Andrew McNeel, and Guohui Li
Center for Atmospheric Chemistry and the Environment
Texas A&M University

January 29, 2005

The preparation of this report is based on work supported by the State of Texas through a Contract from the Houston Advanced Research Center, Texas Environmental Research Consortium and the Texas Commission on Environmental Quality.

Contact information:

John W. Nielsen-Gammon

3150 TAMUS

Texas A&M University

College Station, TX 77843-3150

n-g@tamu.edu

979-862-2248

Table of Contents

| | |
|---------|---|
| Page 3 | Executive Summary: Findings and Recommendations |
| Page 7 | List of Figures |
| Page 10 | Chapter 1: Introduction |
| Page 11 | Chapter 2: Data and Methodology |
| Page 11 | 2a) Data |
| Page 12 | 2b) Method of Estimating Background Ozone |
| Page 19 | Chapter 3: Ozone Climatology |
| Page 19 | 3a) Background Ozone Variability |
| Page 21 | 3b) Background Ozone Climatology |
| Page 23 | 3c) Background, Local Contribution, and Total Ozone |
| Page 25 | 3d) Meteorological Correlates with Ozone |
| Page 29 | Chapter 4: Principal Component Analysis |
| Page 37 | Chapter 5: Principal Components and Background Ozone |
| Page 37 | 5a) The Relationship Between Principal Components and Ozone |
| Page 41 | 5b) PC1 as a Predictor of Background Ozone |
| Page 45 | 5c) Lagged PC1 as a Predictor of Background Ozone |
| Page 51 | Chapter 6: Results |
| Page 52 | References |

Executive Summary: Findings and Recommendations

Key findings and recommendations of general interest are in **boldface**. Page numbers are shown in [brackets].

From Chapter 1:

1. As has been done by TCEQ, it is useful to consider the daily ozone levels in a particular area as being the sum of two quantities: the background ozone and the local contribution. (page 10)

2. The background ozone is defined as the ozone level that would be attained if there were no local anthropogenic (or unusual biogenic) emissions of ozone precursors. (page 10)

3. The local contribution is the difference between the 8-hour maximum background ozone and the 8-hour maximum actual ozone. (page 10)

From Chapter 2:

4. The lowest 8-hour maximum cannot be taken to be the background ozone level in Dallas-Fort Worth (DFW) or Houston-Galveston-Brazoria (HGA) because the lowest maximum is often found in the urban core or other sites affected by local emissions. (page 13)

5. A particular limited set of stations, assumed to be measuring pristine ozone under appropriate wind conditions, is used in DFW and HGA for estimating the background ozone in those two areas. (page 13-14)

6. Individual stations within the limited set typically, but not always, record the lowest 8-hour ozone when the wind blows from the station toward the metropolitan area. (page 15-19)

7. Other regions had few monitors, so none were excluded. (page 15)

From Chapter 3:

8. Taking DFW as an example, there is year-to-year variability in the timing and magnitude of peaks of background ozone, but its interannual variability is sufficiently small that a multi-year average is an appropriate measure of typical conditions. (page 19)

9. Day-to-day variability of background ozone can be a factor of two or more, especially during late summer and early fall. (page 20)

10. There is relatively little variability of background ozone during the winter and during occasional periods in the early summer. (page 20)

11. The regular annual variation is a fundamental component of background ozone. (page 20)

12. All regions of eastern Texas have the same basic pattern of annual variation of background ozone. Background ozone is low in December but starts rising steadily in mid-January. A secondary maximum of background ozone is reached in mid-May, followed by a period with lower ozone values. The overall maximum in each region occurs in August or September, followed by a decline through the fall. (page 21-22)

13. Northeast Texas (NETX) appears to have the highest background ozone concentrations through the year. (page 22)

14. Differences in background ozone between NETX and DFW suggest that, because of sampling problems, absolute background ozone levels cannot be compared between regions with many sensors and regions with few sensors. (page 22)

15. DFW reaches a relative minimum in background ozone around the end of June and an absolute maximum in late August, while HGA reaches a relative minimum in early July and an absolute maximum in mid-September. (page 23)

16. The decline in ozone during the summer is largest in the southern regions and smallest in the northern regions. (page 23)

17. Background ozone levels as computed by the present method are suspiciously low at Beaumont-Port Arthur, suggesting that the sampling network has local source issues. (page 23)

18. The local contribution at DFW makes up less than a third of the total 8-hour ozone maximum on average days. (page 24)

19. The local contributions at DFW and HGA peak in July and August. (page 24-25)

20. The local contribution at HGA is generally a greater percentage of the total ozone than at DFW and reaches an average value of 0.035 ppmv in August. (page 25)

21. The local contribution at HGA averages 0.010 ppmv greater than at DFW, while the background at HGA averages 0.010 ppmv less than at DFW, leading to similar mean 8-h ozone levels. (page 25)

22. Background ozone levels at HGA and DFW correlate most strongly with the wind direction (and component from the north) on the previous day, with slightly lower but still highly significant correlations on the same day and two days previous. (page 26)

23. Also contributing to background ozone are weak winds at HGA and a lack of precipitation at DFW. (page 27)

24. The local contribution at DFW and HGA is positively correlated with high temperatures, low wind speeds, and a lack of precipitation. (page 27)

25. On days without precipitation, the average 8-h maximum ozone in HGA in early September exceeds the 8-h standard. Ozone in DFW comes close. (page 28)

From Chapter 4:

26. Principal Component Analysis (PCA) is useful for representing the large-scale winds, which may be expected to strongly control background ozone, as a small number of continuously-varying patterns. (page 30)

27. Mean ozone-season winds are from the southeast in the HGA area and from the south in the DFW area, rotating clockwise around a center of high pressure in the southeastern United States. (page 31)

28. The leading principal component (PC1), which explains the greatest amount of variability in the wind pattern, represents winds from the southwest (if positive) or northeast (if negative). It therefore is an indicator of the presence (or absence, if positive) of transport from the central and eastern United States. (page 31)

29. The second principal component (PC2) is positive with winds from the northwest. (page 31-32)

30. The total wind on any given day is the sum of the mean wind and the daily amplitudes of the various principal components. (page 33)

From Chapter 5:

31. The principal component most strongly correlated with background ozone is PC1, followed by PC5 and PC2. (page 37)

32. The correlations are strongest with the wind pattern one day before the ozone event. (page 37)

33. By itself, PC1 explains background ozone variations of about 0.017 ppmv at DFW and over 0.020 at HGA. (page 38)

34. The mean value of PC1 declines steadily from spring to fall, consistent with the expected increasing prevalence of continental transport in late summer and early fall. (page 41)

35. The intraannual variation of PC1 explains the early fall background ozone peak, but does not explain why spring experiences higher background ozone than early summer. (page 42)

36. PC1 is much less variable in the summer, so days with PC1 less than -8 (favorable for high background ozone) are somewhat more common in spring than summer. The summer sees extended periods of onshore transport. (page 42)

37. Even with a given wind pattern (PC1), background ozone levels are higher by close to 0.010 ppmv in spring than in early fall. (page 43)

38. The PC1 values on two days together are a better predictor of background ozone than a single-day PC1 value. This finding is consistent with the expectation that extended transport from the continent is more favorable for high background ozone than single days with favorable winds. (page 45)

39. Winds from the southwest carry high ozone if they were recently from the northeast. (page 46)

40. At given values of PC1 at zero and two-day leads, background ozone in HGA is 0.010 ppmv to 0.018 ppmv higher in spring than in summer. This suggests that the relatively high background ozone in springtime high regardless of the day-to-day weather patterns. (page 47)

41. Previous research suggests that high springtime ozone values are a consequence of the high lifetime of ozone in spring combined with a wintertime buildup of NO_x. (page 48-49)

42. DFW background ozone is less sensitive to details of transport than HGA background ozone. (page 49)

List of Figures

Figure 2.1: Scatterplot of u and v for all days in which station CAMS 31, located north of DFW, experienced the lowest maximum 8-h ozone. (page 16)

Figure 2.2: Scatterplot of u and v for all days in which station CAMS 94, located south of DFW, experienced the lowest maximum 8-h ozone. (page 17)

Figure 2.3: Scatterplot of u and v for all days in which station CAMS 78, located north of HGA, experienced the lowest maximum 8-h ozone. (page 18)

Figure 2.4: Scatterplot of u and v for all days in which station CAMS 34, located south of HGA, experienced the lowest maximum 8-h ozone. (page 19)

Figure 3.1: Chart of average background ozone by month in the DFW region, 1994-2003. (page 20)

Figure 3.2: Chart of daily background ozone in the DFW region for years 1998 and 2000. (page 21)

Figure 3.3: Six-year average background ozone in various regions in eastern Texas. Curves in this and later figures are smoothed with a 31-point running mean filter. (page 22)

Figure 3.4: Six-year average local contribution, background, and maximum total ozone at DFW. (page 24)

Figure 3.5: Six-year average local contribution, background, and maximum total ozone at HGA. (page 25)

Figure 3.6: Six-year average local contribution, background, and maximum total ozone at HGA on days without rainfall. (page 27)

Figure 3.7: Six-year average local contribution, background, and maximum total ozone at DFW on days without rainfall. (page 28)

Figure 4.1: Subset of EDAS domain used for principal component analysis (PCA), showing the mean wind field during ozone season (April-October). The bottom wind vector in this and other figures is 5 m/s long. (page 30)

Figure 4.2: The leading two principal components (PC1 and PC2), plotted with amplitude equal to one standard deviation. (page 31)

Figure 4.3: The next two principal components (PC3 and PC4), plotted as in Fig. 4.2. (page 32)

Figure 4.4: Principal components PC5 and PC7, plotted as in Fig. 4.2. (page 33)

Figure 4.5: Wind pattern described by (left) $PC1=-11$, $PC2=8$ ($PC1 = -1$ standard deviation and $PC2 = +1$ standard deviation) and (right) $PC1=-11$, $PC2=-8$. (page 34)

Figure 4.6: Wind pattern described by (left) $PC1=11$, $PC2=8$ and (right) $PC1=11$, $PC2=-8$. (page 35)

Figure 4.7: Wind pattern described by (left) $PC1=0$, $PC2=8$ and (right) $PC1=0$, $PC2=-8$. (page 36)

Figure 4.8: Wind pattern described by (left) $PC1=-11$, $PC2=0$ and (right) $PC1=11$, $PC2=0$. (page 37)

Figure 5.1: Mean background ozone in DFW as a function of the PC1 coefficient (with zero lead). (page 39)

Figure 5.2: Mean background ozone in HGA as a function of the PC1 coefficient. (page 39)

Figure 5.3: Frequency histogram of PC1 coefficients. (page 40)

Figure 5.4: 31-point running mean of daily average PC1 values. (page 41)

Figure 5.5: Plot of PC1 values throughout the ozone season. (page 43)

Figure 5.6: Background ozone values in Houston, by season, as a function of PC1. (page 44)

Figure 5.7: Background ozone values in Dallas-Fort Worth, by season, as a function of PC1. (page 44)

Figure 5.8: Background ozone values as a function of PC1 with 1-day lead and PC1 with no lead. (page 45)

Figure 5.9: Background ozone values as a function of PC1 with 2-day lead and PC1 with no lead. (page 46)

Figure 5.10: The difference between the April-May background ozone and June-July background ozone in HGA, as a function of PC1 with 2-day lead and PC1 with no lead. (page 48)

Figure 5.11: Background ozone in DFW as a function of PC1 with one-day lead and PC1 with zero lead. (page 50)

1. Introduction

The new federal standard for ozone restricts the average concentration of ozone over an eight-hour period to 0.08 parts per million (ppm). This standard must be achieved by the three-year average of the fourth-highest daily maximum eight-hour ozone concentration at any particular monitor. The two obvious differences are the averaging period (longer) and the allowed concentration (smaller). In the previous standard, the one-hour limit could be exceeded at a particular station no more than three times in a three-year period. With the new eight-hour standard, based upon an average, there is no single event that establishes the amount by which a metropolitan area exceeds (or complies) with the standard.

One consequence of this new standard is that ozone must be understood on a broader, interannual basis. One very bad year does not have as great an impact in the eight-hour standard as with the one-hour standard. Indeed, ozone levels in a good year are just as important as ozone levels in a bad year, because it is the average of the good and bad years that determines possible violations of the standard.

The purpose of this two-part study is to develop a conceptual model for eight-hour ozone exceedances in the Houston-Galveston (HGA) metropolitan area. For a variety of reasons, it is useful to consider the daily ozone levels in a particular area as being the sum of two quantities: the background ozone, defined as the ozone level which would be attained if there were no local anthropogenic emissions of ozone precursors, and the local contribution, defined as the difference between the 8-hour maximum background ozone and the 8-hour maximum actual ozone. This approach, first applied in Texas by the Texas Commission on Environmental Quality (TCEQ) has conceptual as well as practical advantages. Conceptually, such an approach is useful for understanding how meteorology contributes to high ozone levels, since the processes that lead to high background levels differ in important ways from the processes that lead to high local contributions. Practically, any control strategies must take into account the amount by

which ozone can be reduced by local controls versus the amount that can be expected to be transported in from other areas and possibly be modified by remote controls.

This report, the first of two parts, considers the climatology and meteorology of background ozone levels in eastern Texas. Although the ultimate goal of these reports is to understand eight-hour ozone exceedances in particular metropolitan areas, background ozone levels tend to rise and fall somewhat in tandem throughout eastern Texas. Thus, the report will simultaneously consider background ozone from northeast Texas to Corpus Christi, including the Dallas-Fort Worth (DFW) metropolitan area.

Section 2 describes the data sources and the method for estimating background ozone and local contributions. Section 3 describes the ten-year climatology of eight-hour (8-h) ozone in eastern Texas, with respect to background exceedances and local contributions. Section 4 describes the principal component analysis (PCA) of transport winds during ozone season (April-October) and relates the PCA components to observed wind patterns. Section 5 describes the relationship between background ozone and wind patterns using PCA. Section 6 summarizes the results.

2. Data and Methodology

2a) Data

The ozone data for this study was downloaded from the Environmental Protection Agency's (EPA) Air Quality System (AQS) database, accessed via the web site <http://www.epa.gov/ttn/airs/airsaqs/detaildata/downloadaqdata.htm>. The full period of record of hourly ozone observations on the web site, from 1994 to 2003, was downloaded in July 2004.

Additional preliminary ozone data was obtained from the TCEQ web site http://www.tnrcc.state.tx.us/cgi-bin/monops/8hr_monthly for 2004.

The surface meteorological data from the TCEQ network was obtained from the TCEQ web site, and surface meteorological data from the hourly weather observing network was obtained from the National Climatic Data Center (NCDC). The period covered by the surface data is January 1999 through June 2003.

The gridded meteorological analyses were created by the National Meteorological Center (NMC) using the Eta Data Assimilation System (EDAS). The analyses were obtained from an archive at the National Center for Atmospheric Research (NCAR) that stores the EDAS analyses on a 40 km grid. The analyses were retrieved for the months of April through October, 1998-2004 (the final two months of 2004 were not yet available as of this writing).

2b) Method of Estimating Background Ozone

Bryan Lambeth and Pete Breitenbach at TCEQ have developed the concept of background ozone as the amount of ozone that would be present without local emissions sources. We find this approach useful and adopt it here.

A sophisticated approach to estimating background ozone is presently in use at TCEQ. This approach involves determining the transport wind direction and selecting as an appropriate background concentration the highest 8-h ozone concentration observed at an appropriate rural site upwind of the metropolitan area of interest.

The TCEQ approach is inherently accurate but also somewhat subjective and labor-intensive. A simpler approach would be to compute the highest 8-h ozone concentration at each of the monitors in a region and assign as the background value the lowest 8-h maximum ozone concentration observed at any sensor. Both approaches assume that monitors are sufficiently broadly distributed about a metropolitan area that at least one sensor will always be uninfluenced by local emissions.

The simpler approach is attractive for its simplicity, but is subject to error when monitors close to concentrated emissions sources experience depressed ozone levels because of the high concentrations of young precursors. The problem is illustrated by computing the percentage of observations at each monitor that represent the lowest 8-h ozone maximum in the entire region. In DFW, the most common lowest ozone occurrences are at the stations closest to and downstream of the Dallas urban core. In HGA, the situation is somewhat more complex.

The station that is most likely to have the lowest 8-h maximum ozone in HGA is CAMS 407 (Crawford), with a hit rate of 19.1%. The second most likely site is also an urban one, CAMS 408 (Lang), with a hit rate of 17.7%. These two urban sites cannot be measuring low background levels, because they are surrounded by monitors, most more rural, which observed higher 8-h maximum ozone.

Many of the other common low ozone sites are near the perimeter of the observing network. One might presume that the best background sites would be Galveston (with a nearly pristine fetch from the Gulf of Mexico) and Conroe (under northerly or northeasterly wind conditions). However, to the south, both CAMS 11 (Clute, 17.5%) and CAMS 10 (Texas City, 12.7%) are much more likely to have the lowest ozone than CAMS 34 (Galveston, 1.9%). CAMS 10 is an unlikely background site, since it is in the immediate vicinity of extensive petrochemical refining. CAMS 11 is more plausible, but it too is immediately downwind of a major plant under the prevailing wind direction. So it appears that even the more rural monitors are subject to local contamination of background ozone readings.

In order to use stations that truly sample background ozone values, we have specified a limited set of stations from which background ozone levels can be estimated in DFW and HGA (Table 1). In DFW, these stations are chosen because they are reasonably distant from the core metropolitan areas and are distributed throughout the range of compass directions relative to DFW. The most distant stations are not selected because spatial variations of background ozone would cause a low bias in the background

ozone estimates, as some stations would experience ozone lower than what was approaching DFW. In HGA, we have selected all of the perimeter stations except CAMS 10 and CAMS 11.

Table 1: Stations included in the estimate of background ozone levels in HGA and DFW.

| EPA Number | CAMS | Description | Period Used |
|--------------------------|-------------|--------------------------|-------------------------------------|
| Houston/Galveston | | | |
| 48-201-0066 | 410 | Westhollow | all |
| 48-201-0051 | 409 | Croquet | all |
| 48-201-0029 | 26 | NW Harris Co. | all |
| 48-339-0078 | 78 | Conroe Relocated | all |
| 48-339-0089 | 65 | Conroe | all |
| 48-167-0014 | 34 | Galveston | all (installed 11/1/96) |
| 48-039-1016 | 11 | Clute | through 10/31/96 |
| Dallas/Fort Worth | | | |
| 48-113-0087 | 402 | Dallas Executive Airport | 4/04-7/16/96; 10/1/96-8/27/97 |
| 48-085-0005 | 31 | Frisco | all |
| 48-397-0001 | 69 | Rockwall Heath | all |
| 48-139-0015 | 94 | Midlothian Tower | 7/17/96-9/30-96; 8/28/97-present |
| 48-257-0005 | 71 | Kaufman | all |
| 48-439-1002 | 13 | Fort Worth NW | through 6/5/00 |
| 48-439-0075 | 75 | Eagle Mtn. Lake | since 6/6/00 |
| 48-251-0003 | 77 | Cleburne | all |

The monitoring network was smaller during the early part of the 1994-2003 period, and with some network configurations there was no monitor in certain upstream directions. In those cases, the best available upstream monitor was used, even if that

monitor may have been affected by local emissions. Thus, Clute is used in HGA until Galveston was installed, Dallas Executive Airport is used in DFW when Midlothian Tower was not installed, and Fort Worth NW is used in DFW until Eagle Mtn. Lake was installed. Since 2000, no such compromises were necessary.

In the other five regions considered here, there were typically five or fewer monitors. With this small number, it was necessary to include all stations in the search for background ozone values.

Except where otherwise noted, the data analysis in the remainder of this report is restricted to data from the period 1998-2003, when data coverage was best.

If the lowest 8-h maximum from the selected stations truly measures background ozone, background levels at each station should almost exclusively occur when the wind direction is from the station toward the city. Figures 2.1-2.4 show the occurrence of background ozone at two selected stations in DFW and two in HGA as a function of the u and v components of the wind. Station CAMS 31 (Fig. 2.1) is located north of the DFW area. Although winds are rarely from the north, most background ozone occurrences at that station are associated with winds from the north and northeast. CAMS 94, to the south, is upstream for the prevailing wind direction, and most background occurrences there correspond to a southeast wind. In the Houston area, CAMS 78, north of town, experiences background values when the wind is from the north and northeast, while CAMS 34, southeast of the city, is a common background site under southeast wind conditions. The background ozone appears to be reasonably well-behaved: winds from the north tend to favor stations located to the north, while winds from the south favor stations located to the south.

Wind Components for Background Ozone at CAMS 31

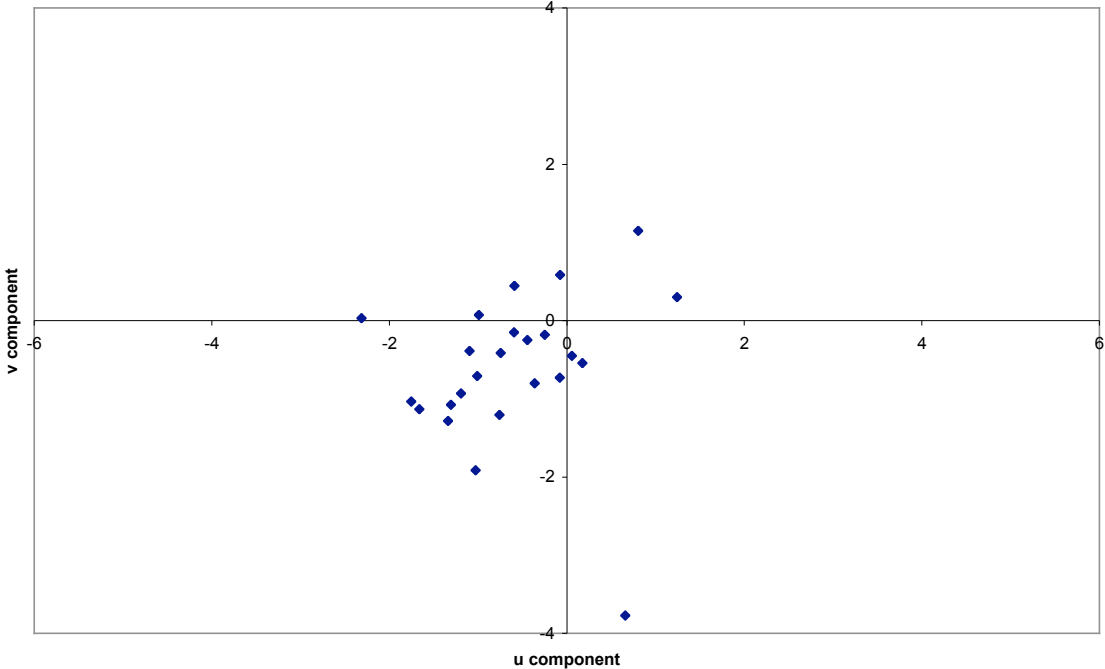


Figure 2.1: Scatterplot of u and v for all days in which station CAMS 31, located north of DFW, experienced the lowest maximum 8-h ozone.

Wind Components for Background Ozone at CAMS 94

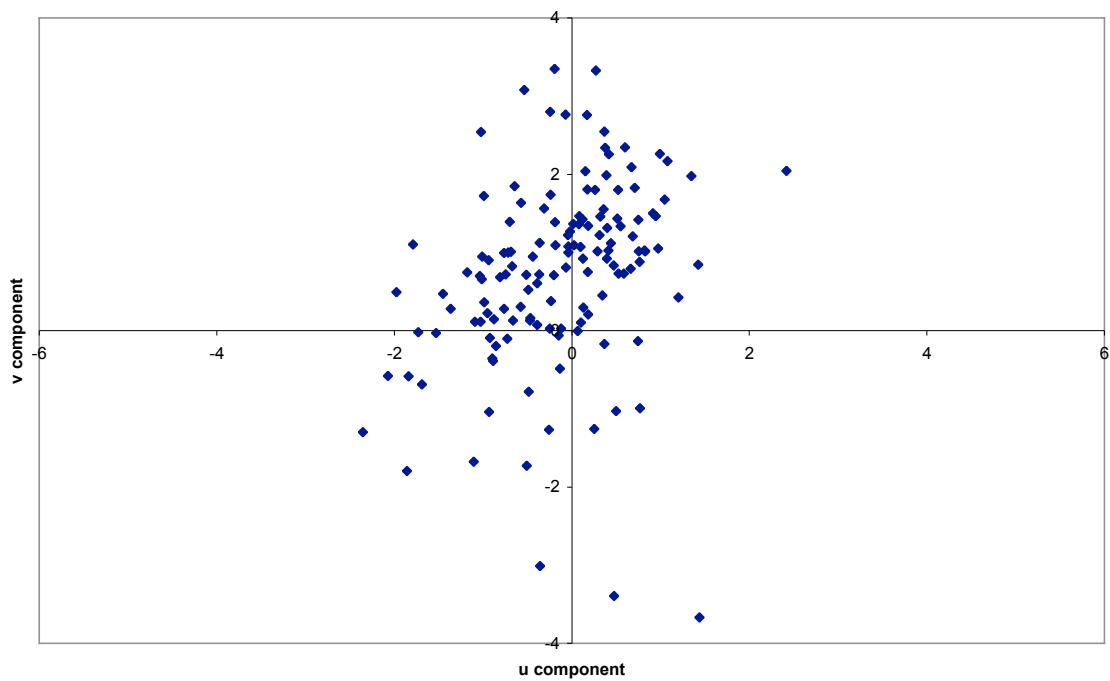


Figure 2.2: Scatterplot of u and v for all days in which station CAMS 94, located south of DFW, experienced the lowest maximum 8-h ozone.

Wind Components for Background Ozone at CAMS 78

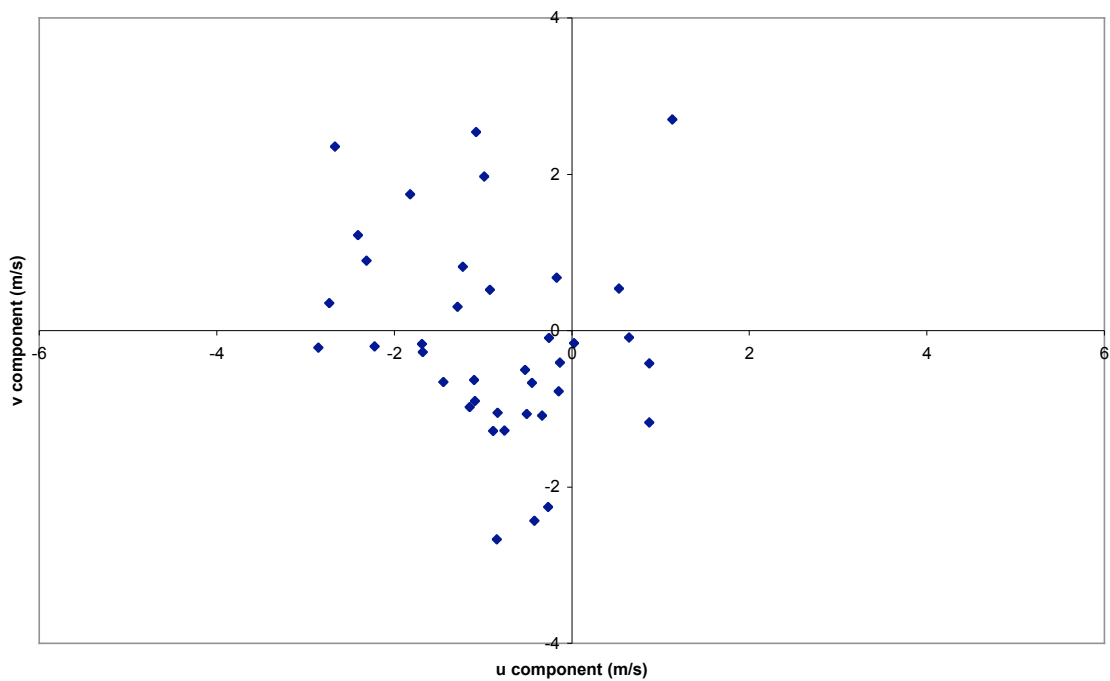


Figure 2.3: Scatterplot of u and v for all days in which station CAMS 78, located north of HGA, experienced the lowest maximum 8-h ozone.

Wind Components for Background Ozone at CAMS 34

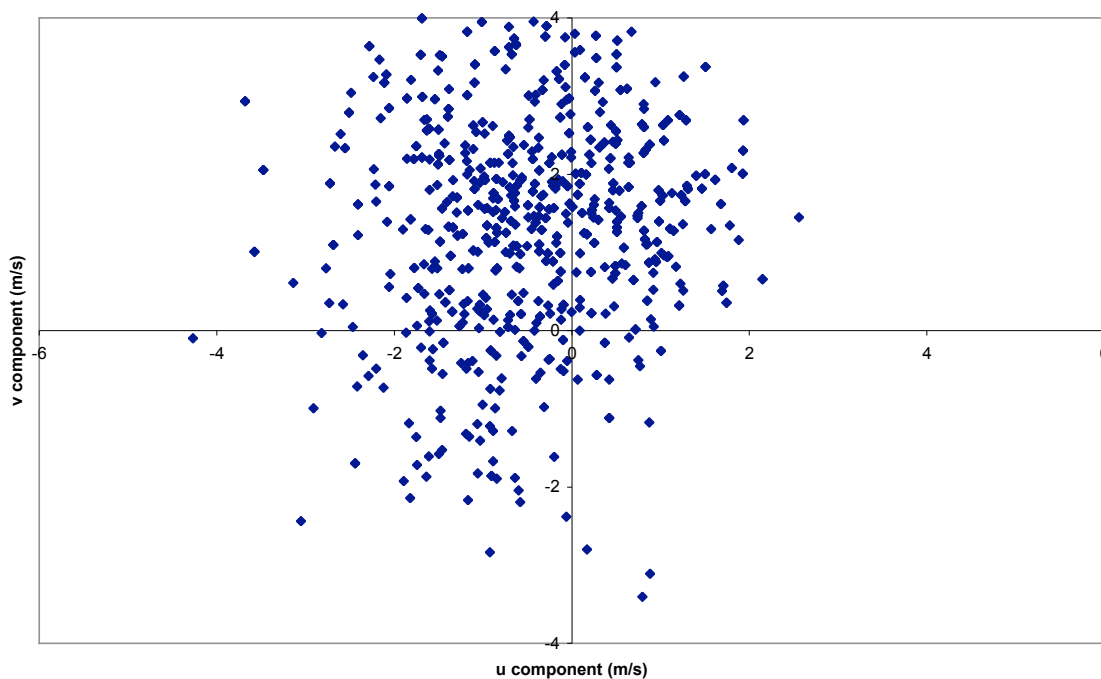


Figure 2.4: Scatterplot of u and v for all days in which station CAMS 34, located south of HGA, experienced the lowest maximum 8-h ozone.

3. Ozone Climatology

3a) Background Ozone Variability

As an example, the monthly average background ozone at DFW from 1994 to 2003 is shown in Fig. 3.1. Certain climatological features are generally present, though they do not necessarily appear every single year. For example, the highest background ozone tends to occur in late summer, with an occasional secondary peak in late spring. The decline in background ozone in the fall is rather abrupt almost every year. Certain periods stand out, such as the spring of 1998 when ozone levels were unusually high or the spring of 2000 when ozone levels were unusually low, but in general it appears that background ozone variations on monthly timescales would be reasonably well represented by conditions averaged over several years.

DFW Monthly Mean Background Ozone

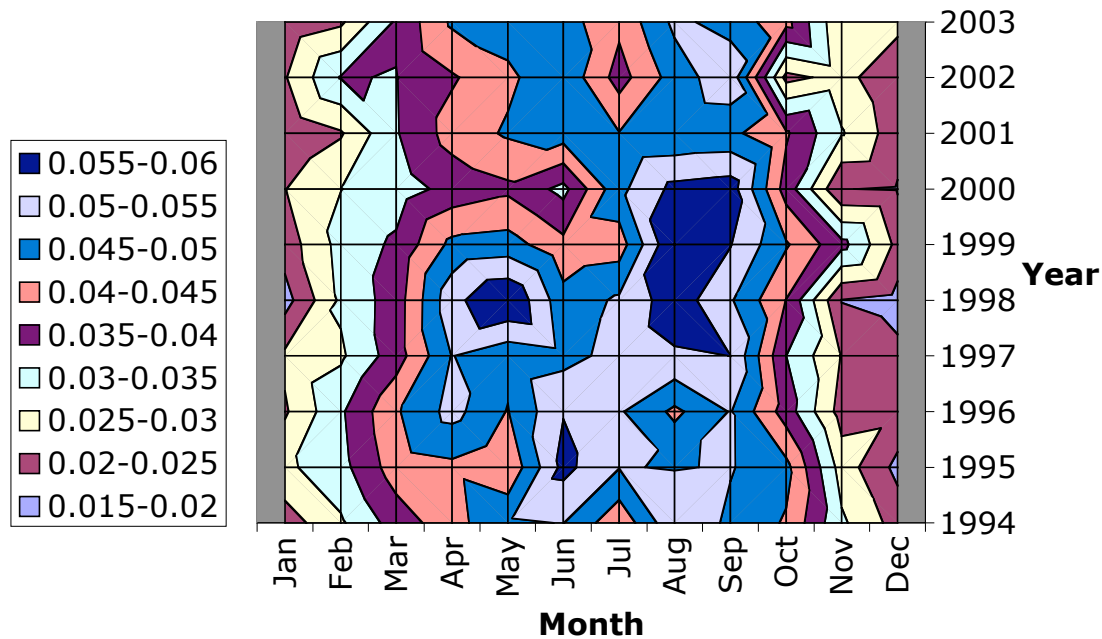


Figure 3.1: Chart of average background ozone by month in the DFW region, 1994-2003.

The monthly averages do mask considerable day to day variability, particularly during the warm season. For example, Fig. 3.2 shows the daily background ozone in 1998 and 2000 in DFW. Variations of background ozone concentration by a factor of two on a daily to weekly time scale are common. The largest variability takes place in late summer and early fall, while the smallest variability occurs during the winter. Both series also exhibit a period in June in which the variability is unusually low.

The 1998 and 2000 background ozone seasons shown in Fig. 3.2 are perhaps the most dissimilar of the ten years of data, especially in springtime. Certainly the daily peaks in ozone in the two years occur in different months. Nonetheless, both years seem to follow the same basic pattern of ozone variation. Collectively, Figs. 3.1 and 3.2 lend support to the idea that the regular annual variation is a fundamental component of background ozone.

DFW Daily Background Ozone

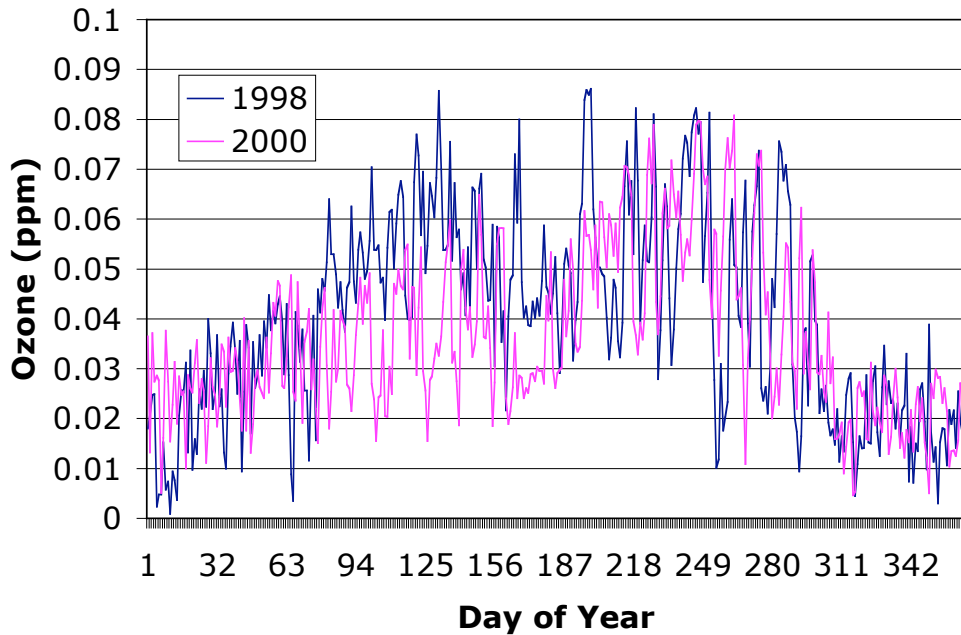


Figure 3.2: Chart of daily background ozone in the DFW region for years 1998 and 2000.

3b) Background Ozone Climatology

The annual variation of background ozone across eastern Texas is shown in Fig. 3.3. Seven regions are included: Dallas-Fort Worth (DFW), Tyler-Longview-Marshall (NETX), Beaumont-Port Arthur (BPA), Austin (AUS), Houston-Galveston (HGA), San Antonio (SAT), and Victoria-Corpus Christi (VCC).

All seven regions have the same basic pattern of annual variation of background ozone. Background ozone is low in December but starts rising steadily in mid-January. A secondary maximum of background ozone is reached in mid-May, followed by a period with lower ozone values. The overall maximum in each region occurs in August or September, followed by a decline through the fall.

Background Ozone, 1998-2003

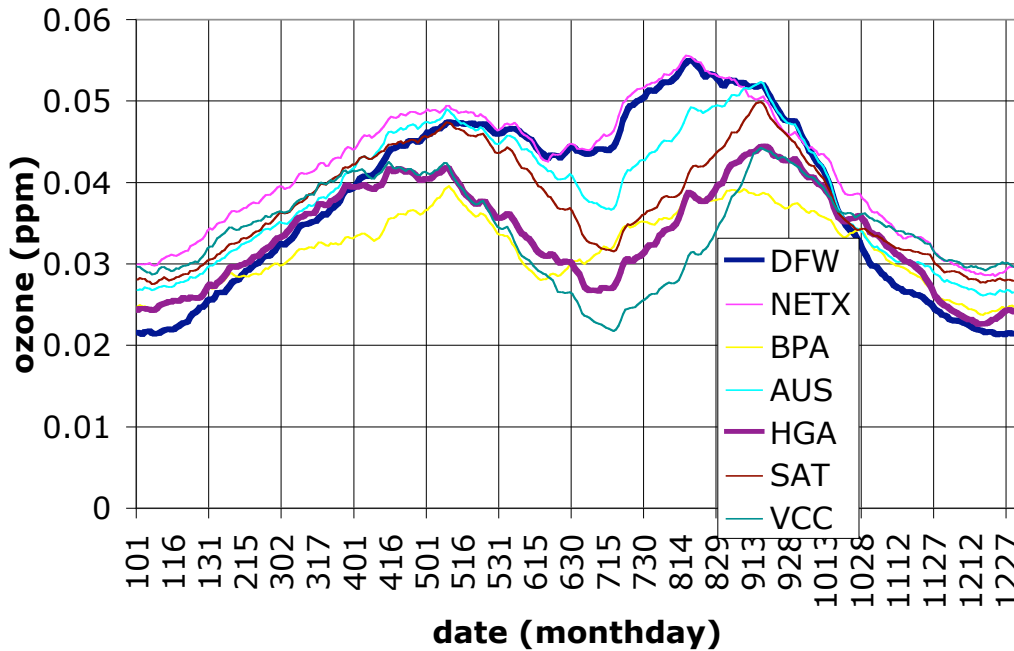


Figure 3.3: Six-year average background ozone in various regions in eastern Texas. Curves in this and later figures are smoothed with a 31-point running mean filter.

The region with the highest background ozone concentrations through the year appears to be NETX. The DFW region is comparable in background ozone levels to NETX during the summertime, but during the rest of the year DFW is lower than NETX by about 6-8 ppb. We are aware of no meteorological or photochemical reason why background ozone levels should be substantially lower in DFW than NETX during most of the year, including some periods in which NETX is highest and DFW lowest throughout eastern Texas. We conclude that these differences are artifacts caused by applying the background ozone estimation technique to regions with widely varying numbers of stations and levels of urbanization. Because of these sampling differences, it is inappropriate to directly compare the background ozone magnitudes in heavily-instrumented and less-instrumented regions simultaneously.

The two populous (well-sampled, but heavily urbanized) regions are DFW and HGA. The two exhibit similar background ozone levels during the winter and early

spring, climbing from 0.02-0.025 ppm around the New Year to 0.04-0.045 ppm by mid-April. Beyond mid-April, the two curves diverge. HGA begins a decline in background ozone that bottoms out in early July at levels almost as low as those at the beginning of the year, while DFW continues rising to mid-May and declines only to about 0.043 ppm around the end of June. DFW then climbs to a peak of 0.055 ppm in late August, while HGA does not reach its background peak of 0.044 ppm until mid-September. By mid-October DFW background ozone has fallen to HGA levels, and the two continue to decline rapidly for the rest of the year.

The other five regions vary in a similar manner, with a continuous gradation in the ozone climatology from northeast to southwest. The spring peak occurs latest at NETX and earliest at VCC. The decline in ozone during the summer is largest in the southern regions and smallest in the northern regions. The summer minimum of background ozone occurs latest and is most pronounced in VCC and is earliest and least pronounced in DFW and NETX. The minimum in mid-summer is so strong at VCC that the background ozone levels in mid-summer there are considerably lower than the background ozone levels in mid-winter. The late summer maximum is earliest at DFW and NETX and latest at VCC.

The outlier from this pattern is BPA. At various times throughout the year, particularly when background ozone levels are high, the BPA background levels are much lower than would be expected from the trends in surrounding regions. Perhaps background ozone at BPA is being scavenged by local sources near the monitors.

3c) Background, Local Contribution, and Total Ozone

If a small number of stations adversely affects the estimation of background ozone, it must seriously harm the estimation of local contribution. Therefore, we only consider the local contributions in DFW and HGA.

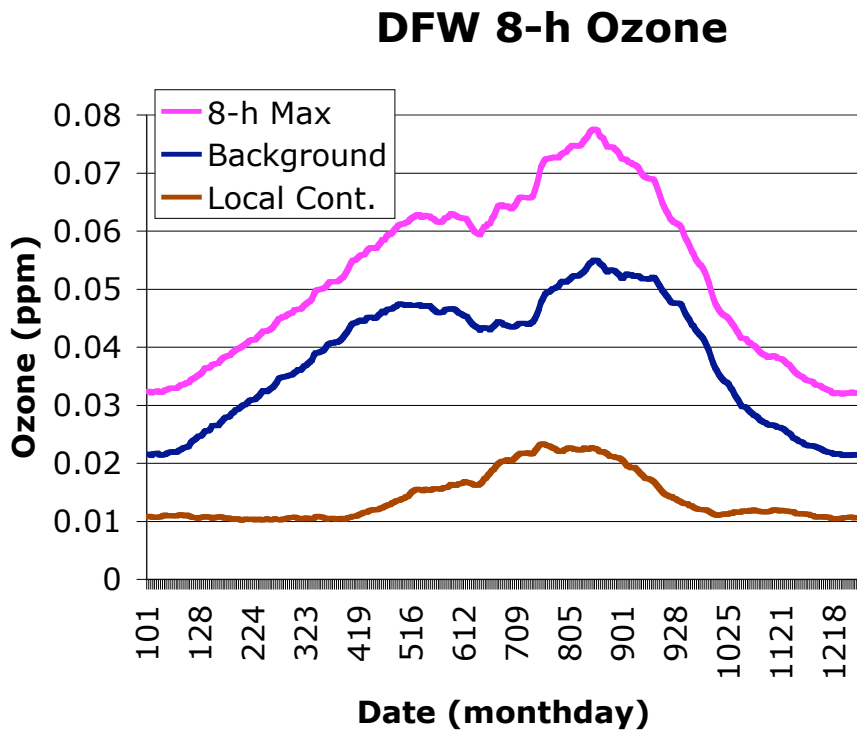


Figure 3.4: Six-year average local contribution, background, and maximum total ozone at DFW.

The components of average maximum 8-h ozone at DFW are shown in Fig. 3.4. The local contribution, on average, is a relatively insignificant component of DFW’s 8-h maximum ozone, contributing less than a third of the total ozone. (The local contribution might nevertheless be more significant on extreme ozone days.) The peak local contribution occurs in mid-July, when temperatures are highest and solar radiation is strong. Because the peak local contribution is nearly in phase with the early summer minimum in background ozone, the 8-h maximum ozone does not have a pronounced early summer minimum.

The components of average maximum 8-h ozone at HGA are shown in Fig. 3.5. Unlike at DFW, a midsummer minimum is retained in the 8-h maximum ozone at HGA. The background ozone levels in spring and fall are almost identical. The peak local contribution in early August leads to the 8-h maxima being shifted closer to mid-summer than the background maxima: the spring 8-h maximum is nearly a month later than the

background ozone maximum, while the late summer 8-h maximum is nearly a month earlier than the background peak.

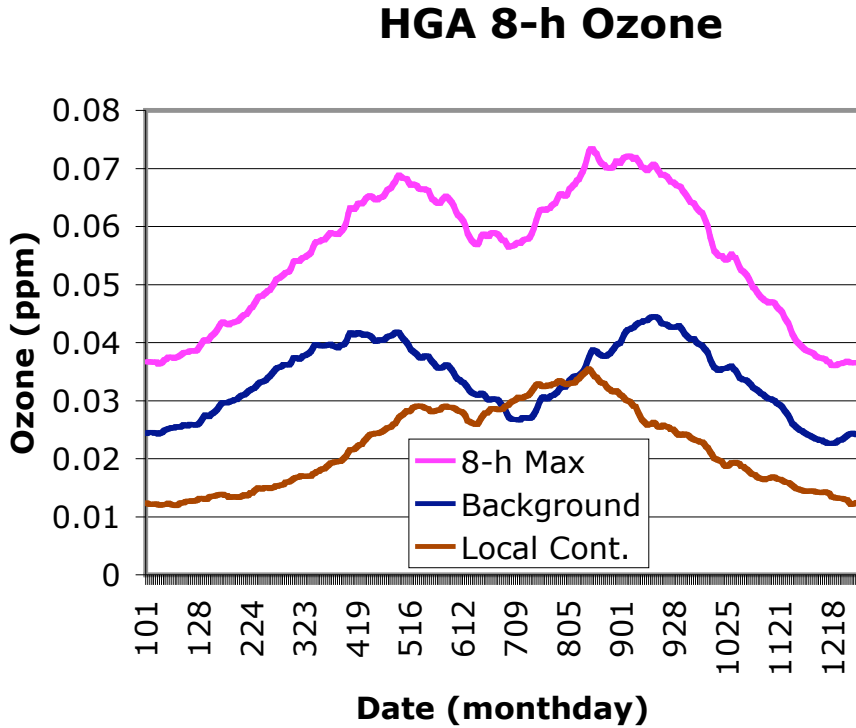


Figure 3.5: Six-year average local contribution, background, and maximum total ozone at HGA.

The local contribution is about 0.01 ppm larger at HGA than at DFW. Roughly speaking, this makes up for background ozone values which during the summer are about 0.01 ppm larger at DFW than HGA, yielding comparable mean daily 8-h ozone maxima.

3d) Meteorological Correlates with Ozone

For an initial assessment of the meteorological and external factors that control the variations in background ozone and local contributions, correlations were computed

with respect to 58 possible predictors, involving wind, temperature, rainfall, day of week, and day of year. The results are shown in Table 2.

Table 2: Strongest meteorological correlations with ozone. Meteorological parameters ending with a 0, 1, or 2 correspond to the day of the ozone event, the day prior to the ozone event, and two days prior to the ozone event, respectively. sinD and cosD are the sine and cosine of the direction of the 24-h mean wind, u and v are the components of wind toward the east and north, spd is the wind speed, isX is 1 if the wind is from the X direction and 0 otherwise, binp (binpt) is 1 if there was measurable (measurable or a trace) precipitation during the 24-hour period and 0 otherwise (or during the afternoon six-hour period if indicated by “6h”), and tmp is the maximum temperature.

| HGA | | DFW | | HGA | | DFW | |
|-------------------|-------|-------------------|-------|--------------|-------|--------------|-------|
| Background | | Background | | Local | | Local | |
| cosD1 | .578 | cosD1 | .470 | tmp0 | .478 | tmp0 | .374 |
| v1 | -.538 | v1 | -.462 | spd0 | -.358 | spd0 | -.306 |
| cosD2 | .501 | v2 | -.433 | binpt0 | -.335 | spd1 | -.291 |
| v0 | -.483 | cosD2 | .428 | binp0 | -.320 | isS1 | -.247 |
| cosD0 | .469 | binpt0 | -.381 | binp6ht0 | -.314 | isS0 | -.228 |
| v2 | -.445 | isS1 | -.361 | spd1 | -.304 | v1 | -.220 |
| isS0 | -.391 | binp0 | -.351 | u1 | .276 | isS2 | -.198 |
| isS1 | -.391 | v0 | -.347 | binp6h0 | -.294 | spd2 | -.195 |
| spd0 | -.384 | cosD0 | .338 | u2 | .231 | binp6ht0 | -.195 |
| spd1 | -.372 | tmp0 | .336 | u0 | .219 | binpt0 | -.193 |
| isNE1 | .358 | isS2 | -.309 | sinD2 | -.200 | binp0 | -.187 |
| isNE2 | .315 | binp6ht0 | -.304 | isSW1 | .193 | v2 | -.186 |

The background ozone levels depend most strongly on the cosine of the previous days' wind direction and the north-south component of wind. For both two parameters, a northerly wind (a wind from the north) favors high background ozone, with direction slightly more important than speed. Northerly winds on other days are also favorable.

Also contributing to background ozone are weak winds at HGA and a lack of precipitation at DFW.

The same-day temperature is most strongly correlated with local contributions to ozone at both HGA and DFW, followed by wind speed, with weak winds favored. Precipitation is also a negative influence, especially at HGA. At DFW a weak south wind strongly favors high ozone, but at HGA the wind component from the west seems to favor high ozone.

The importance of light winds for high local contributions is not surprising. The strong dependence of background ozone on the north-south component of wind is not particularly surprising either: a strong southerly wind is known to typically bring clear maritime air to Texas.

HGA 8-h Ozone on Days Without Precipitation

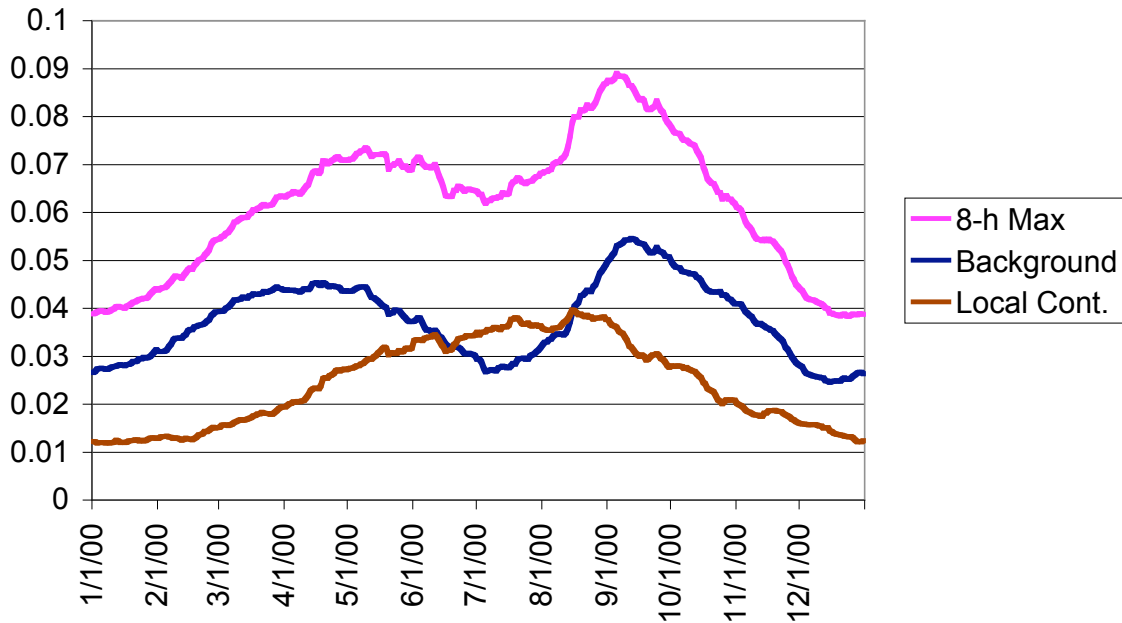


Figure 3.6: Six-year average local contribution, background, and maximum total ozone at HGA on days without rainfall.

In HGA, the elimination of precipitation days causes a dramatic increase in ozone levels during late August and early September (Fig. 3.6). The late summer peak becomes a sharp one, as background ozone is 0.01 ppm higher with rain days excluded. The 8-h ozone maximum is almost entirely due to the background maximum. This peak is so high that on days without rainfall, an average day in HGA in late August and early September exceeds the 8-hour ozone standard.

In DFW, the elimination of precipitation days does not cause so dramatic an increase in ozone levels, because precipitation days are less frequent in DFW than HGA (Fig. 3.7).

DFW 8-h Ozone on Days Without Precipitation

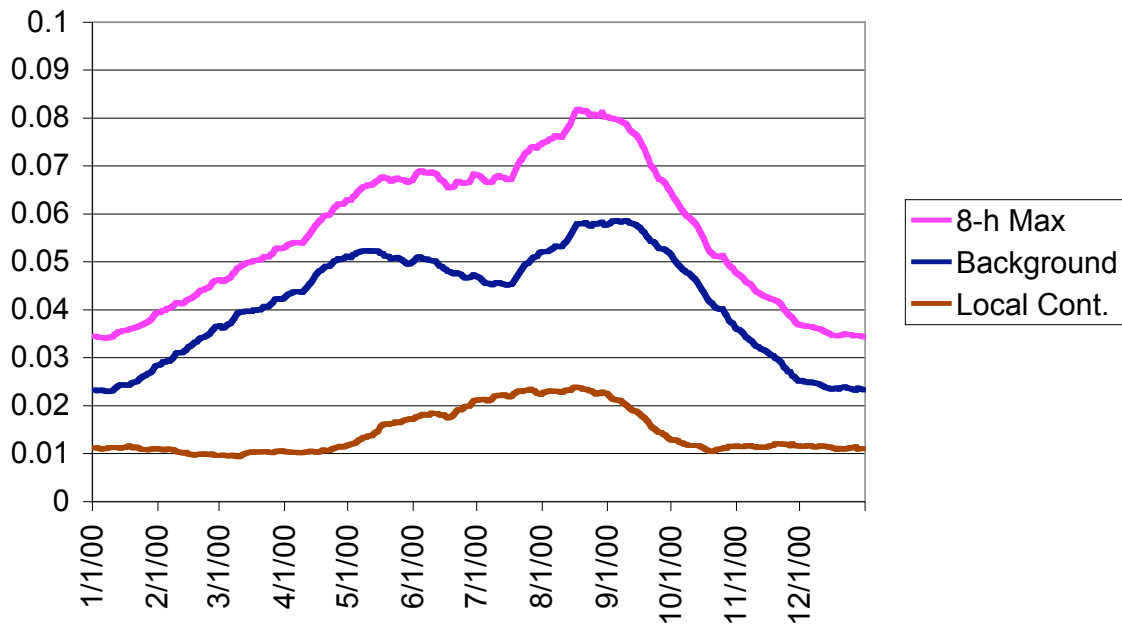


Figure 3.7: Six-year average local contribution, background, and maximum total ozone at DFW on days without rainfall.

Any conceptual understanding of background ozone levels in eastern Texas must explain the late spring peak in background ozone, the midsummer minimum, and the late summer maximum.

4. Principal Component Analysis

Wind patterns and trajectories from the central United States are well known to be associated with high levels of ozone in Texas. However, quantification of this relationship is difficult. Previous investigators have used swarms of trajectories for arbitrarily-defined high-ozone and low-ozone days in an attempt to determine preferred directions of transport. However, this approach is not easily quantified and the proper length of the trajectories is not clear.

An alternative approach would relate the local winds in the region to background ozone levels. However, this approach would be sensitive to the correlation between the local wind and the broader-scale wind pattern. In a sense, the local wind is being used as a proxy for the larger-scale pattern.

The convenience of using the local wind is that the local wind can be described by two variables: either the two wind components, or the wind speed and direction. A complete description of a larger-scale wind field requires $2n$ variables, where n is the number of grid points comprising the larger-scale wind field. The number of dimensions quickly becomes intractable.

Yet another approach, called cluster analysis, seeks to find particular recurring weather patterns and group the observed weather patterns into clusters. This approach is appropriate when there are particular coherent patterns of variability, with the atmosphere rapidly transitioning from one mode to another. But when the atmosphere varies gradually and continuously, as it tends to during the summer in Texas, cluster analysis produces an arbitrary grouping of weather events with little or no underlying physical basis.

One purpose of principal component analysis, or PCA, is to reduce the dimensionality of a large data set into a smaller, more manageable number. PCA finds

the dominant modes of variability of the weather patterns. If the day-to-day variations in weather can be described by a very small number of principal components, or empirical orthogonal functions (EOFs), the evolution of the weather can be easily represented on a graph or set of graphs. Furthermore, it is likely that only a small subset of the principal components will be strongly correlated with ozone levels, leading to even smaller dimensionality.

Based on previous conceptual models and trajectory analysis, we define a subset of the EDAS grid as shown in Fig. 4.1. The grid covers the area from eastern Texas to the lower Mississippi River valley and extends as far north as extreme southwestern Kentucky. The original EDAS grid (not shown) is sampled at every other grid point,

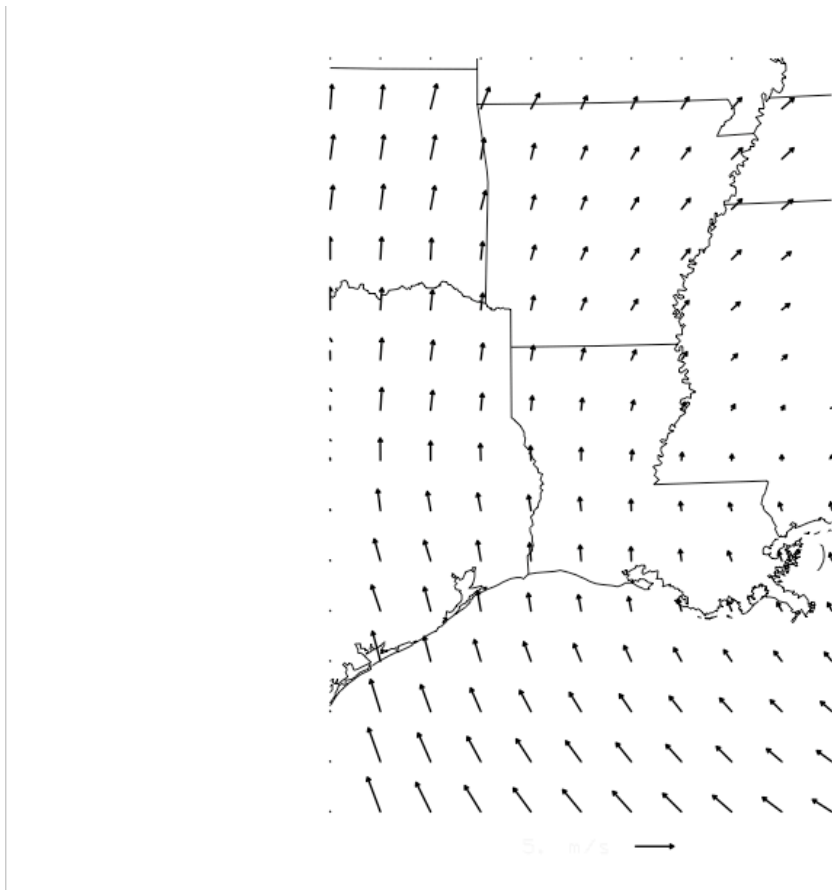


Figure 4.1: Subset of EDAS domain used for principal component analysis (PCA), showing the mean wind field during ozone season (April-October). The bottom wind vector in this and other figures is 5 m/s long.

yielding a grid of 11x16 points. The 925 mb winds (0.5 km to 1.0 km above ground level) were selected as the winds in the transport layer. PCA was then performed on the 1800 UTC (12:00 Noon CST) winds to extract the dominant patterns.

Fig. 4.1 shows the mean winds over the six years of ozone seasons. The wind pattern is dominated by anticyclonic flow around a high pressure center to the east. Flow enters Texas from the south and exits toward the north.

The dominant principal components are plotted in Figs. 4.2-4.4. Fig. 4.2 shows that PC 1, which represents the strongest mode of variability, corresponds in its positive phase to a vector oriented southwest to northeast, which, when added to the mean wind in Fig. 4.1, produces flow from the south or southwest. Also shown in Fig. 4.2 is PC2,

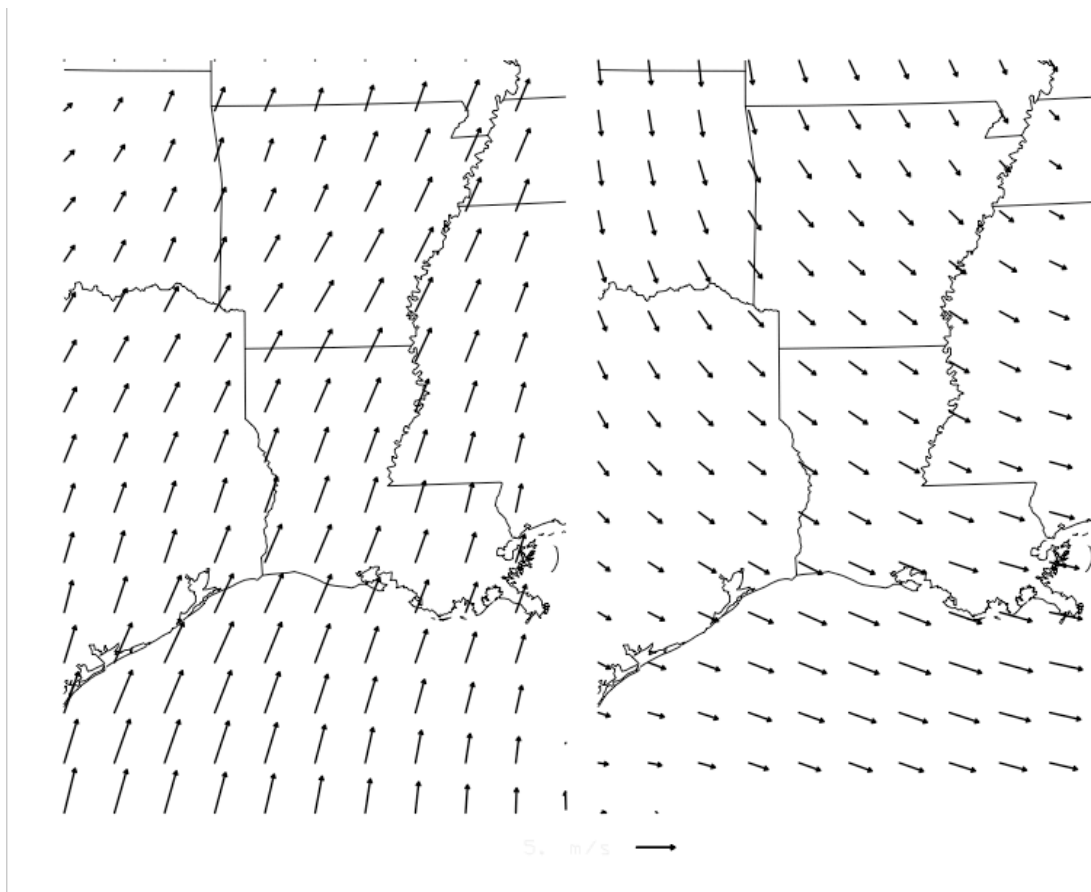


Figure 4.2: The leading two principal components (PC1 and PC2), plotted with amplitude equal to one standard deviation.

which in its positive phase is confluent flow from west to east and in its negative phase is diffluent flow from east to west.

Fig. 4.3 shows PC3 and PC4. PC3 is an anticyclone over the domain when positive and a cyclone when negative. PC4 is a nearly pure deformation field which when positive corresponds to a front oriented northwest-southeast and when negative corresponds to a front oriented northeast-southwest. Together, PC3 and PC4 combine to represent the standard local patterns of nondivergent flow, while PC1 and PC2 can combine to represent the larger-scale wind pattern.

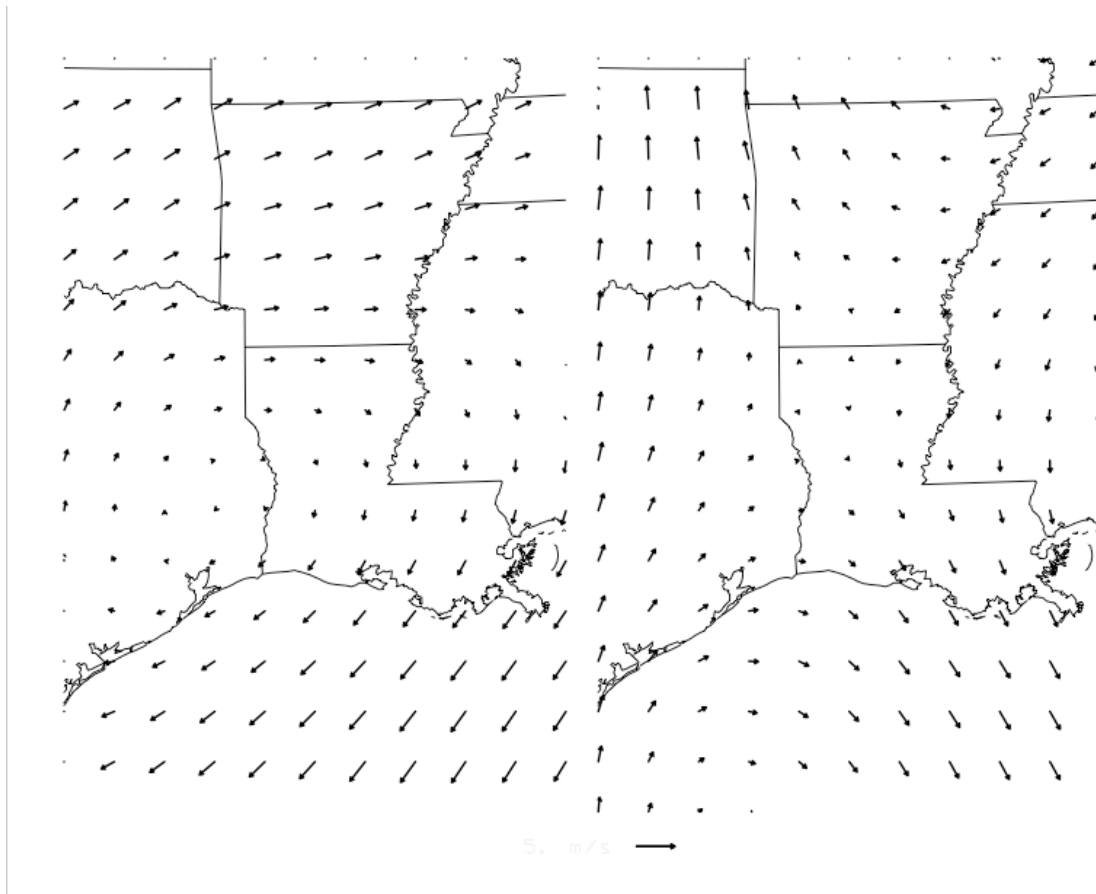


Figure 4.3: The next two principal components (PC3 and PC4), plotted as in Fig. 4.2.

Fig. 4.4 shows the wind patterns for principal components PC5 and PC7. While there is still a somewhat large-scale signal in these principal components, it is weak. The

only principal component beyond PC7 to be highly (negatively) correlated with ozone is a wind pattern that corresponds to convergence in the domain of interest.

The wind pattern on each day can be exactly expressed as the sum of $2 \times 11 \times 16 = 352$ principal components of varying amplitudes. More importantly, the wind pattern can be approximated as the sum of a much smaller set of principal components of varying amplitudes. In fact, the basic large-scale transport patterns can be recovered from just principal components 1 and 2.

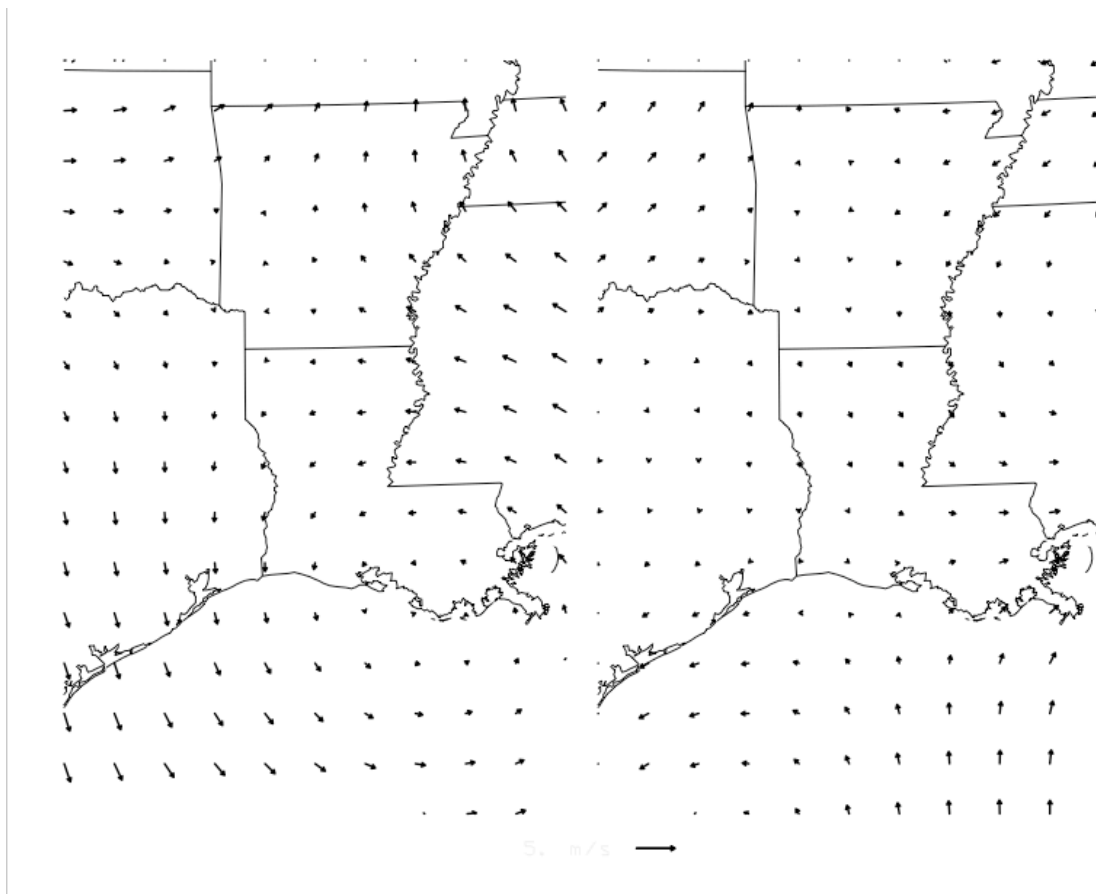


Figure 4.4: Principal components PC5 and PC7, plotted as in Fig. 4.2.

Actual wind patterns on particular days are equal to the mean wind plus the principal component “loadings” for each principal component. Figures 4.5-4.8 show the various wind patterns associated with +/- one standard deviation of various combinations of PC1 and PC2. These plots include the mean wind and assume that all other principal

components are zero. Because of the orthogonality of the principal components, each of the patterns in Figs. 4.7 and 4.8 are equally common, as are (albeit slightly less common) each of the patterns in Figs. 4.5 and 4.6. Most common is the pattern in Fig. 4.1, which consists solely of the mean. Collectively, these wind patterns include predominant wind directions from the southwest, south, southeast, east, northeast, and north.

In the following section, ozone levels will be plotted as a function of PC1, or of PC1 and PC2. The wind patterns provided in this section should be used as reference material showing the two-dimensional wind field associated with particular values of PC1 and PC2.

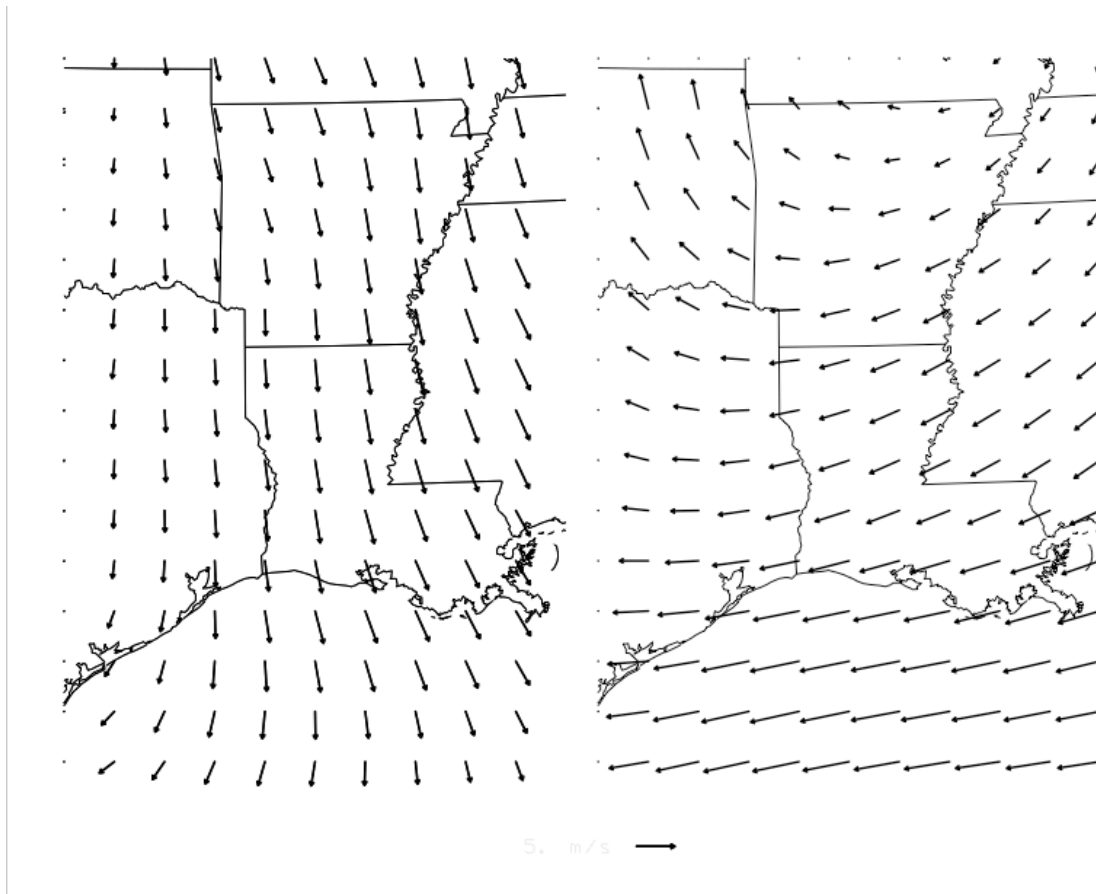


Figure 4.5: Wind pattern described by (left) $PC1=-11$, $PC2=8$ ($PC1 = -1$ standard deviation and $PC2 = +1$ standard deviation) and (right) $PC1=-11$, $PC2=-8$.

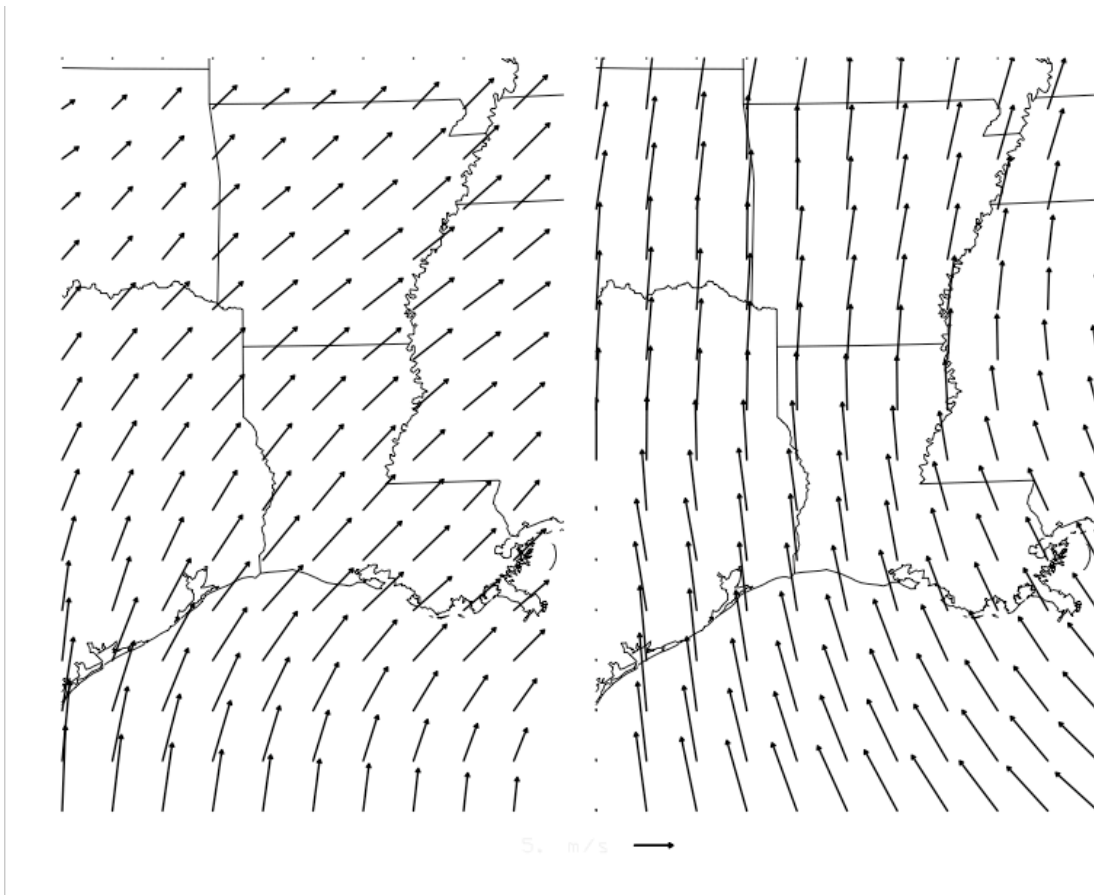


Figure 4.6: Wind pattern described by (left) $PC1=11$, $PC2=8$ and (right) $PC1=11$, $PC2=-8$.

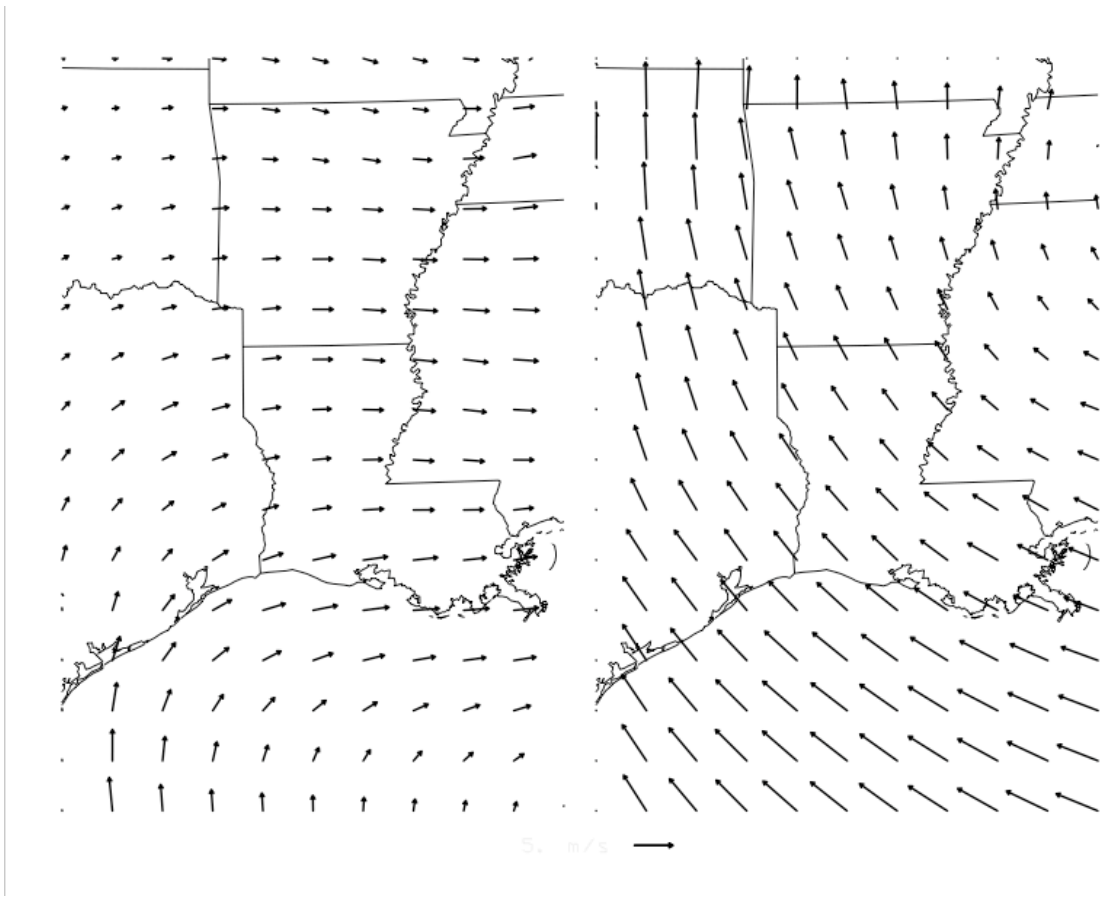


Figure 4.7: Wind pattern described by (left) $PC1=0, PC2=8$ and (right) $PC1=0, PC2=-8$.

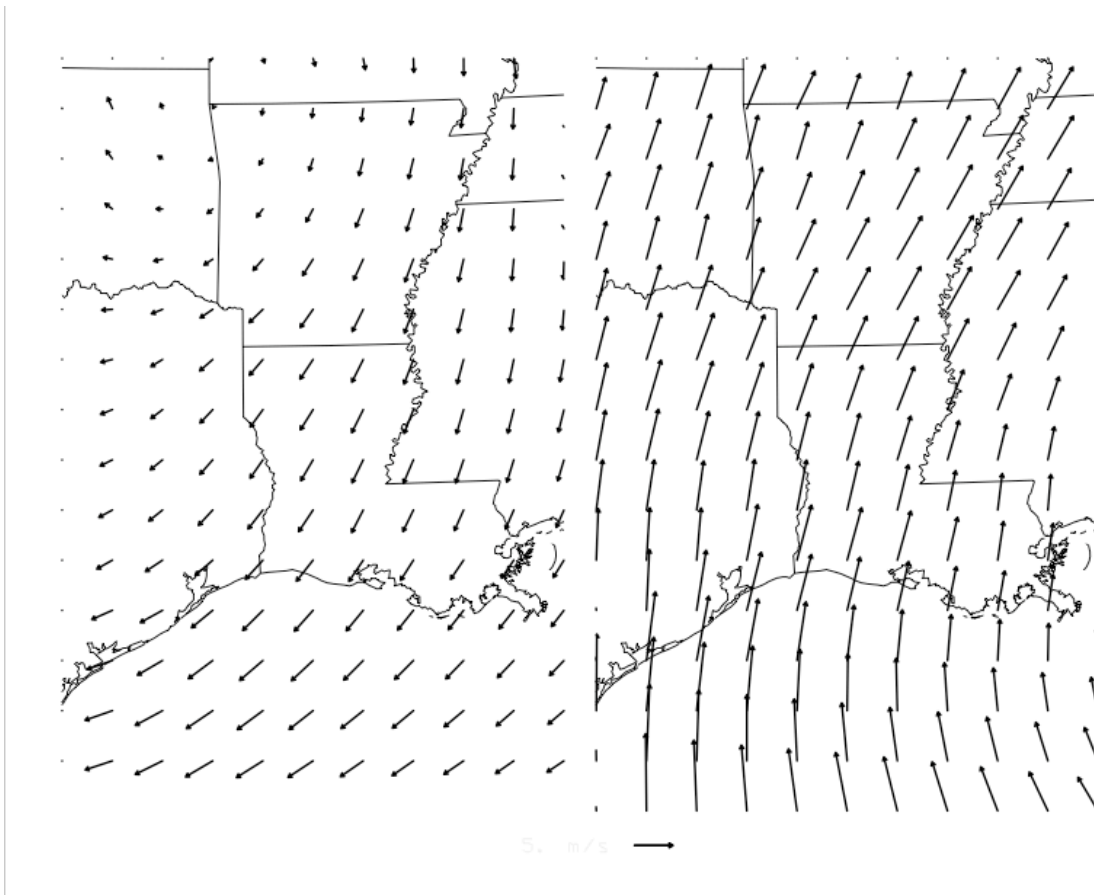


Figure 4.8: Wind pattern described by (left) $PC1=-11$, $PC2=0$ and (right) $PC1=11$, $PC2=0$.

5. Principal Components and Background Ozone

5a) The Relationship Between Principal Components and Ozone

The correlations and significance levels between the various principal components at different lead times and background ozone levels in DFW and HGA are given in Table 3. PC1 is found to be quite highly significant at all three tested lead times, with the greatest significance at a lead of one day. Other principal components, particularly PC5 and PC2, are significantly correlated with one or more ozone parameters, but PC1 is both the dominant wind mode and the dominant controlling factor for ozone.

Table 3: Correlations between principal components at 0, 1, and 2 day lead times with respect to background ozone at Dallas and Houston. The correlations in bold are significant at the 95% confidence level.

| HOUSTON - GALVESTON, 18Z WINDS AND BACKGROUND OZONE | | | | | | |
|---|---------------|--------------|---------------|--------------|---------------|--------------|
| | SAME DAY | | 1 DAY LEAD | | 2 DAY LEAD | |
| | Correlation | P-value | Correlation | P-value | Correlation | P-value |
| PC 1 | -0.369 | 0.000 | -0.417 | 0.000 | -0.334 | 0.000 |
| PC 2 | -0.039 | 0.173 | 0.074 | 0.010 | 0.097 | 0.001 |
| PC 3 | 0.131 | 0.000 | 0.071 | 0.014 | 0.004 | 0.879 |
| PC 4 | 0.057 | 0.046 | 0.020 | 0.482 | -0.003 | 0.931 |
| PC 5 | 0.197 | 0.000 | 0.241 | 0.000 | 0.171 | 0.000 |
| PC 6 | 0.024 | 0.408 | -0.025 | 0.379 | -0.042 | 0.152 |
| PC 7 | 0.062 | 0.032 | 0.013 | 0.654 | -0.009 | 0.756 |
| PC 8 | -0.035 | 0.224 | -0.051 | 0.079 | -0.087 | 0.003 |
| PC 9 | 0.084 | 0.003 | 0.003 | 0.911 | -0.065 | 0.026 |
| PC 10 | 0.029 | 0.308 | -0.051 | 0.078 | -0.052 | 0.071 |

| DALLAS - FORT WORTH, 18Z WINDS AND BACKGROUND OZONE | | | | | | |
|---|---------------|--------------|---------------|--------------|---------------|--------------|
| | SAME DAY | | 1 DAY LEAD | | 2 DAY LEAD | |
| | Correlation | P-value | Correlation | P-value | Correlation | P-value |
| PC 1 | -0.317 | 0.000 | -0.353 | 0.000 | -0.294 | 0.000 |
| PC 2 | 0.085 | 0.003 | 0.207 | 0.000 | 0.215 | 0.000 |
| PC 3 | 0.038 | 0.188 | 0.014 | 0.635 | -0.016 | 0.592 |
| PC 4 | 0.108 | 0.000 | 0.061 | 0.034 | 0.077 | 0.008 |
| PC 5 | 0.199 | 0.000 | 0.217 | 0.000 | 0.169 | 0.000 |
| PC 6 | 0.029 | 0.320 | -0.035 | 0.227 | -0.080 | 0.006 |
| PC 7 | 0.117 | 0.000 | 0.080 | 0.005 | 0.008 | 0.772 |
| PC 8 | 0.026 | 0.362 | -0.015 | 0.614 | -0.032 | 0.275 |
| PC 9 | 0.098 | 0.001 | 0.053 | 0.068 | -0.013 | 0.662 |
| PC 10 | 0.002 | 0.936 | -0.024 | 0.414 | -0.046 | 0.112 |

Despite the strong correlation, the relationship between background ozone and PC1 is not a linear one. Figures 5.1 and 5.2 show the mean background ozone as a function of the PC1 amplitude for DFW and HGA, respectively. In DFW, PC1 by itself can explain variations of background ozone from 0.038 ppm to 0.054 ppm, comparable in magnitude to the season variations of ozone. In HGA, the difference is even more pronounced: positive values of PC1 are associated with ozone below 0.03 ppm, while negative values approach or even exceed 0.05 ppm.

Mean DFW Background O₃ vs PC1

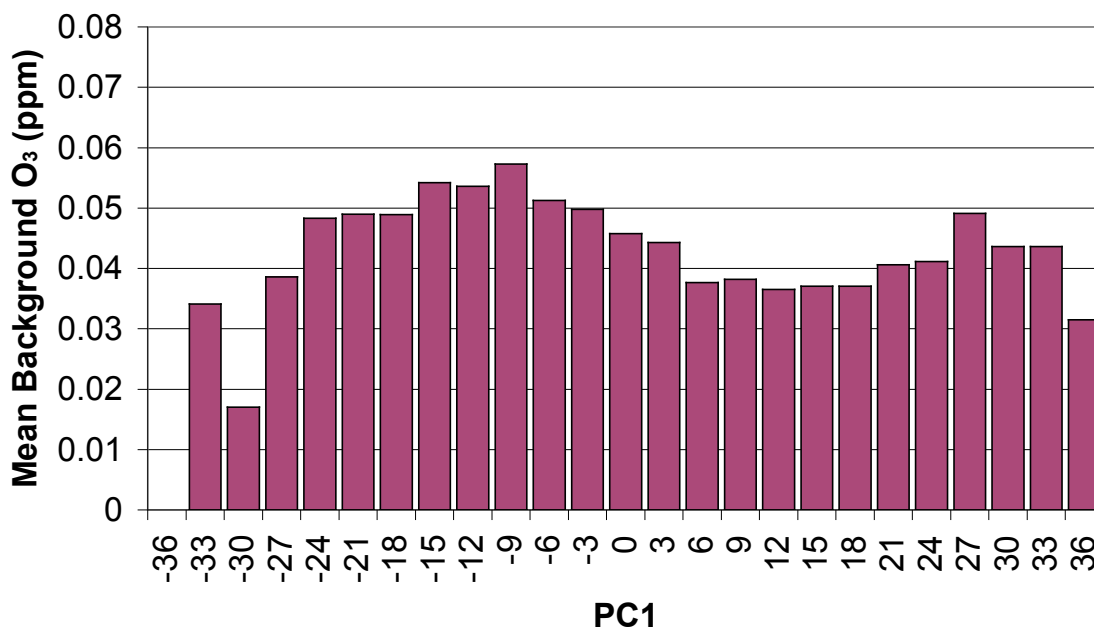


Figure 5.1: Mean background ozone in DFW as a function of the PC1 coefficient (with zero lead).

Mean HGA Background O₃ vs PC1

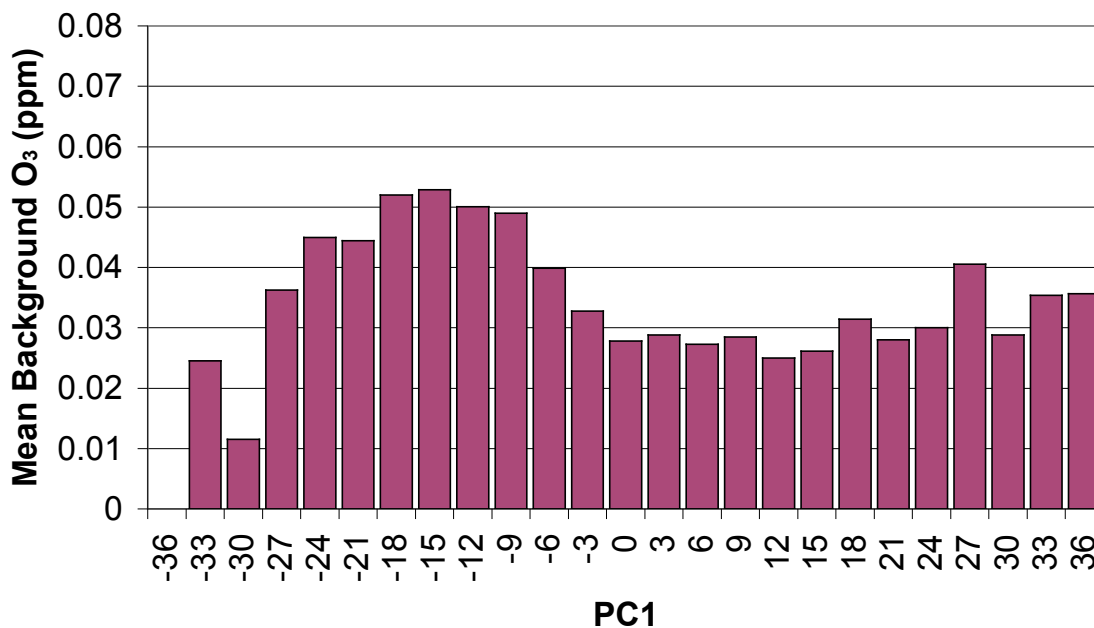


Figure 5.2: Mean background ozone in HGA as a function of the PC1 coefficient.

In both DFW and HGA, the highest background ozone levels are found when the value of PC1 is close to -1 standard deviations from zero (a value of ± 11). A sense of the wind field associated with that value of PC1 is given by examination of Fig. 4.5, which shows PC1 at -1 standard deviation and PC2 and ± 1 standard deviation. Most events with PC1 at -1 standard deviation will lie between the two extremes given by Fig. 4.5a and Fig. 4.5b.

Other principal components (not shown) have comparatively little association with background ozone levels.

Keep in mind when viewing this and other charts that the distribution of PC1 coefficients is normal and centered at 0 with a standard deviation of 11.1 (Fig. 5.3). Very few cases occur at the tails of the distributions.

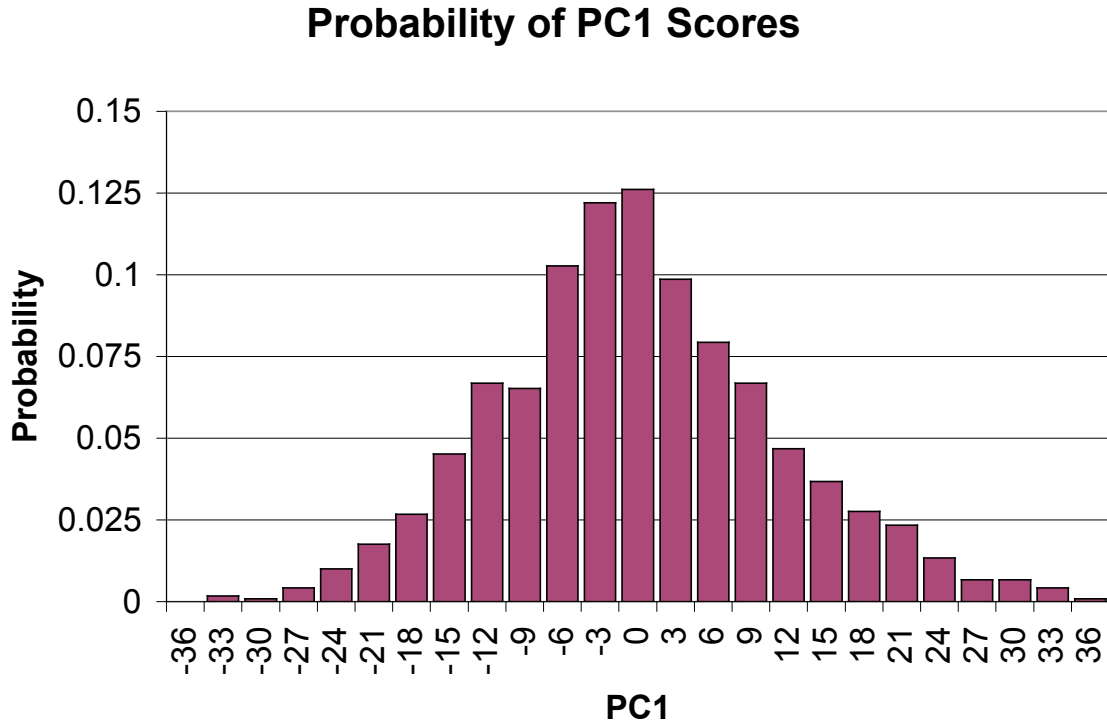


Figure 5.3: Frequency histogram of PC1 coefficients.

5b) PC1 as a Predictor of Background Ozone

Is the observed yearly cycle of background ozone associated with seasonal changes in the background wind? The standard explanation for the late summer maximum of total ozone is a decrease in the intensity of the Bermuda High and a resulting decrease in the strength of onshore flow. This explanation, while plausible, does not on its surface explain the other two maxima and minima of the seasonal ozone cycle.

The mean variation of PC1 through the ozone season is shown in Fig. 5.4. PC1 is largest in April (implying, according to the right side of Fig. 4.8, moderate southwesterly winds). The value of PC1 decreases almost linearly with time through the summer, reaching zero (implying the wind pattern of Fig. 4.1) in July, and approaching -8 (implying the wind pattern of Fig. 4.8 (left)) by the end of September before again rising.

31 Day Running Average of PC1 During Ozone Season

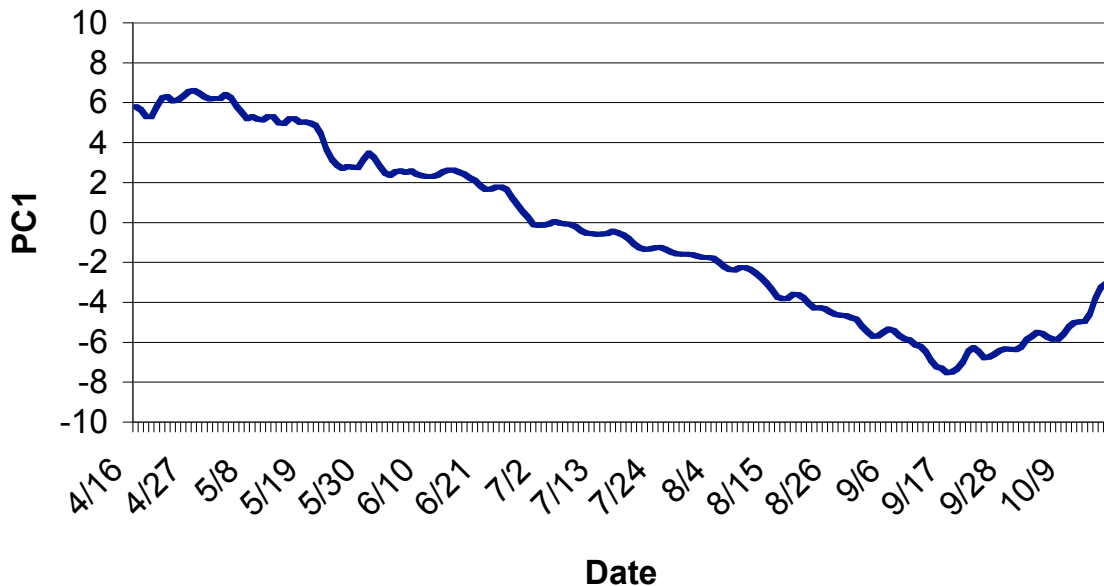


Figure 5.4: 31-point running mean of daily average PC1 values.

The change of PC1 from midsummer values near zero to late summer values near -8 appears to be adequate to explain the change in mean background ozone during this period. In DFW, ozone increases by 0.01, and the change in mean DFW background as PC1 changes from 0 to -8 is similar to this amount. In HGA, too, the ozone increase of 0.02 is comparable to the change in mean HGA background as PC1 changes from 0 to -8 . It is therefore tempting to conclude that the variation of ozone during the latter half of the year is explained by changes in the value of PC1, that is, a weakening of the Bermuda High.

This hypothesis is easily tested, and it turns out that while the hypothesis can explain the increase in background ozone at the end of the summer, it cannot explain the decrease in background ozone at the beginning of the summer.

The next hypothesis considers the fact that weather is much more variable in spring in Texas than in the summer. If summertime PC1 values remain near 0 while springtime PC1 values are highly variable and frequently are strongly negative, it would be possible for average springtime background ozone to be higher than average summertime background ozone.

The scatter of PC1 values through the year is shown in Fig. 5.5. The figure confirms that the variability of the wind field is much smaller in summer than in the other two seasons. However, PC1 dropping below -8 is nearly as common in spring as in the summer. Thus, the PC1 day-to-day variability is sufficient to explain why summer might be similar in background levels to spring, but not why it might be lower.

Suppose that there is an aspect of background ozone unrelated to regional meteorological conditions? If so, a given meteorological situation (PC1 value) would produce a different background ozone value in some seasons compared to others.

Observed PC1 Values vs. Date, Ozone Season

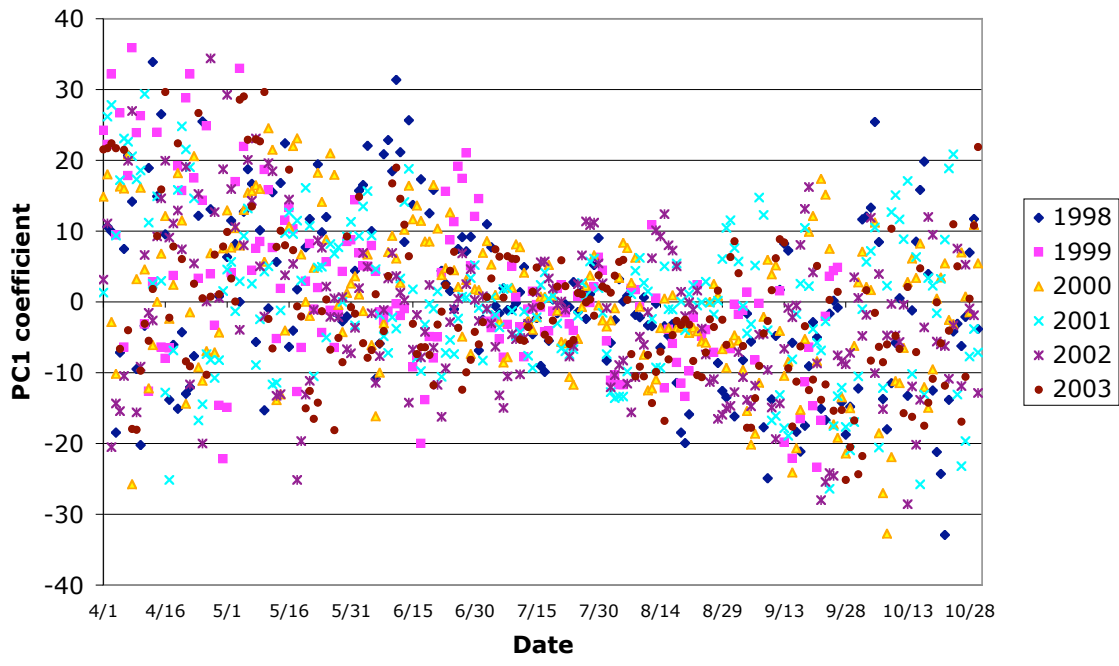


Figure 5.5: Plot of PC1 values throughout the ozone season.

To test this idea, Fig. 5.6 shows the mean background ozone variation in Houston-Galveston as a function of PC1, by month. For most of the range of the principal component, the Apr-May background ozone concentrations are about 0.01 ppm larger than in the other months. This elevated background ozone in spring is insufficient to explain the late spring maximum.

A similar plot for Dallas-Fort Worth (Fig. 5.7) exhibits a similar seasonal cycle but with less amplitude. The DFW plot in particular emphasizes the fact that the dependence of high ozone on PC1 is stronger in summer and fall than in spring.

Mean HGA Background O₃ vs PC1, by Months

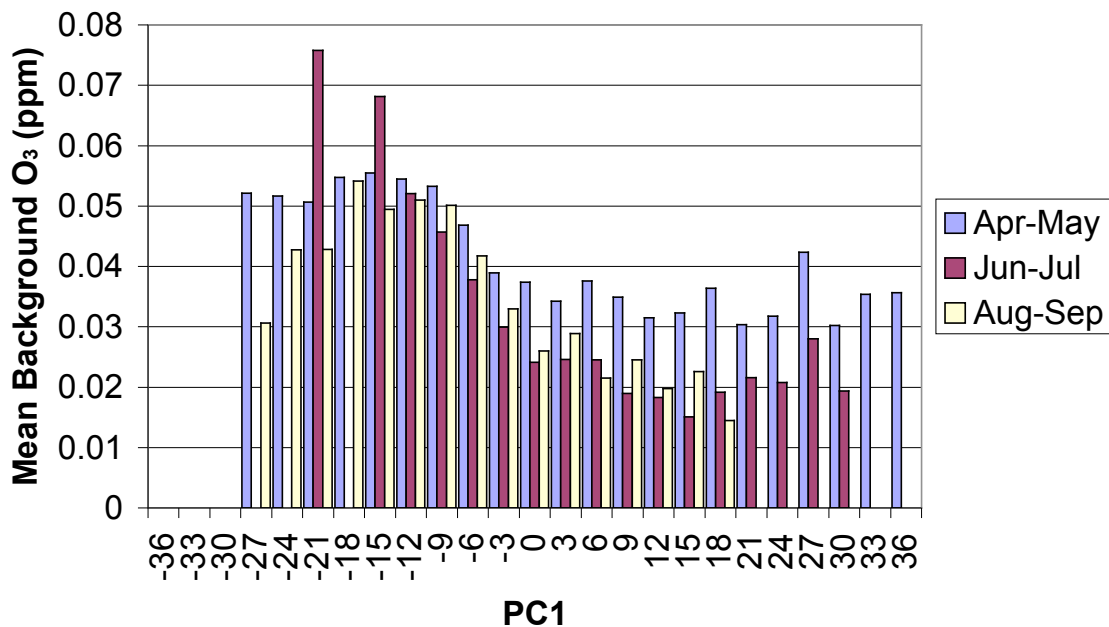


Figure 5.6: Background ozone values in Houston, by season, as a function of PC1.

Mean DFW Background O₃ vs PC1, by Months

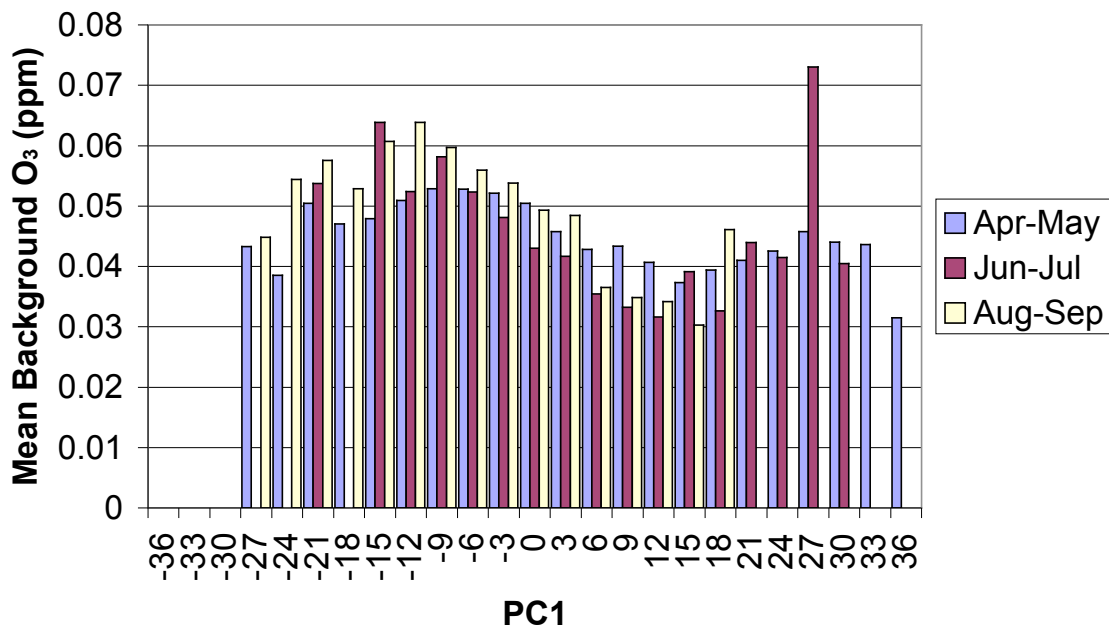


Figure 5.7: Background ozone values in Dallas-Fort Worth, by season, as a function of PC1.

5c) Lagged PC1 as a Predictor of Background Ozone

One reason that ozone levels for a given PC1 value in Aug-Sep might be higher than in Apr-May could be that the rapidly-changing weather patterns in Apr-May could inhibit long-range transport of polluted air to Texas. To examine whether a favorable PC1 on successive days leads to higher background ozone levels, Fig. 5.8 shows the average background ozone at HGA as a function of zero-lead PC1 and one-day lead PC1.

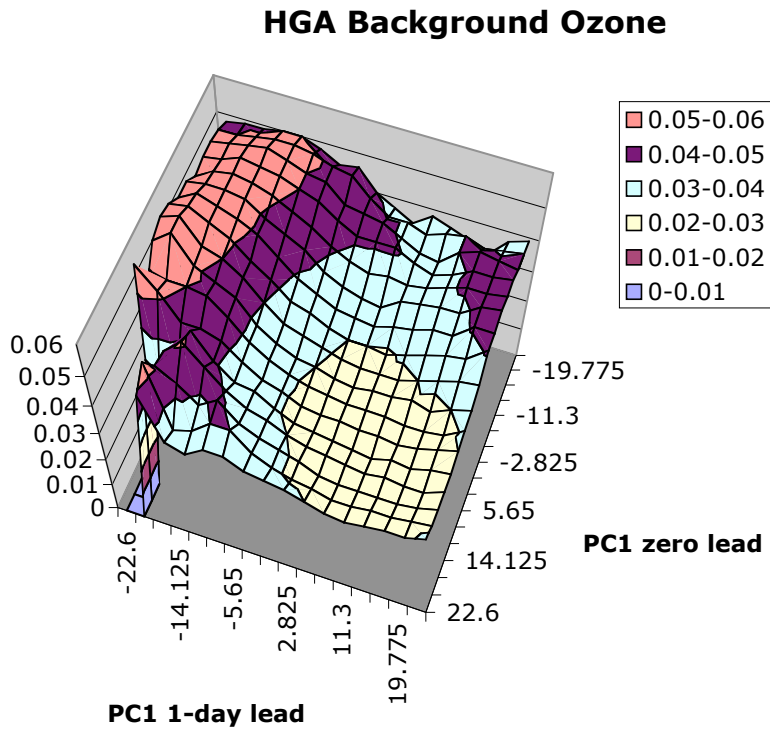


Figure 5.8: Background ozone values as a function of PC1 with 1-day lead and PC1 with no lead.

Compared to Fig. 5.2, there is more variability explained by the two parameters (zero-lead PC1 and one-day lead PC1) than by zero-lead PC1 by itself. If both days have positive PC1, the background ozone averages less than 0.03 ppm. If the previous day's PC1 was strongly negative (transport from the northeast), almost any zero-lead PC1 will be associated with ozone greater than 0.04 ppm.

If two successive days of northeast flow are conducive to high background ozone, what about three successive days? Assuming that the wind rarely, if ever, switches from the northeast and back again on successive days, this question can be addressed with a plot of background ozone as a function of two-day lead PC1 and zero-lead PC1 (Fig. 5.9). The dependence of background ozone is even stronger than in Fig. 5.8, with larger areas below 0.03 ppm and above 0.05 ppm. According to this plot, three successive days of northeasterly transport lead to background ozone well above 0.05 ppm in HGA.

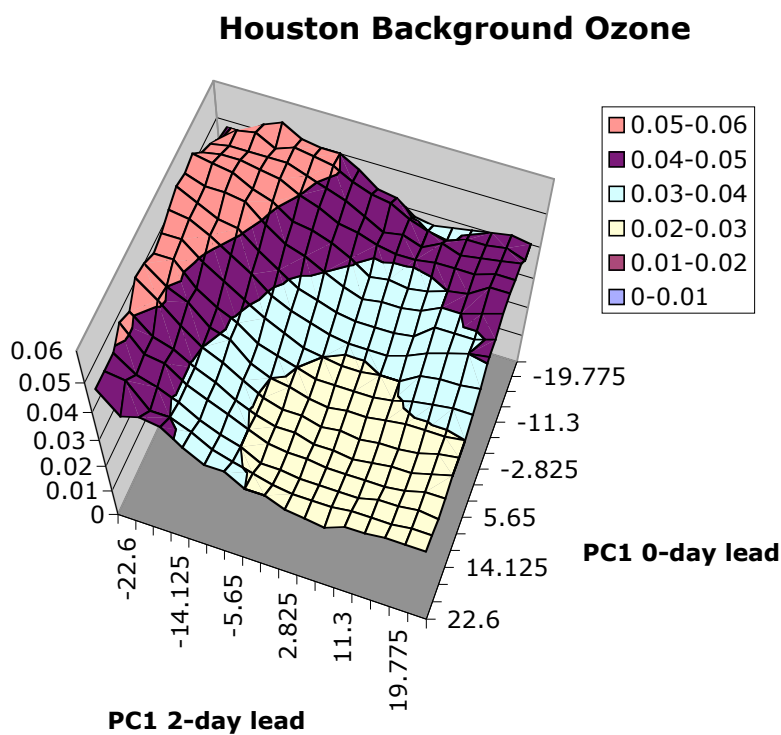


Figure 5.9: Background ozone values as a function of PC1 with 2-day lead and PC1 with no lead.

Note in Fig. 5.9 that a strongly-negative 2-day lead PC1 value is favorable for relatively high background ozone even if 0-day lead PC1 is strongly positive. Transport winds from the northeast that later reverse to southwesterly carry high-background ozone over Houston twice: once coming, and once going. This observation corroborates the

statistical analysis that showed that the wind direction most important to background ozone is observed on days prior to the background ozone level.

The predictive power of this chart is impressive, but variations of PC1 still do not explain the springtime background ozone maximum. Heretofore, the difference between PC1 values in April-May and in June-July has accounted for less than 0.01 ppm, too small to explain the observed April-May maximum. But now that the two-day lead plot (Fig. 5.9) predicts so much of the background ozone variability, we can use this information to *control for the effect of transport variations*.

Figure 5.10 shows the difference between spring and summer background ozone at various combinations of PC1 with a 2-day lead and PC1 with zero lead. Compared to Fig. 5.9, the values are remarkably uniform. Furthermore, except for the rare events along the margins of Fig. 5.10, any given combination of 2-day lead PC1 and 0-day lead PC1 is associated with 0.010 to 0.018 ppmv more background ozone in April-May than in June-July. Assuming that other principal components, which are known to have both lower amplitude and lower correlation with background ozone, cannot account for this difference, one can conclude that a given weather and transport pattern is associated with about 0.012-0.015 ppmv higher background ozone in spring than in summer.

The cause of this spring surplus of background ozone cannot be photochemistry, because the solar insolation is greater in June and July. Similarly, the cause cannot be less cloudiness and precipitation, because April and May are as wet or wetter than June and July. A similar springtime ozone maximum has been observed at rural stations and in the free troposphere throughout the Northern Hemisphere (for a review, see Monks 2000), and the decreased sensitivity of background ozone to wind pattern in springtime is consistent with a hemispheric-scale background ozone signal.

HGA Background Ozone Difference (AprMay-JunJul)

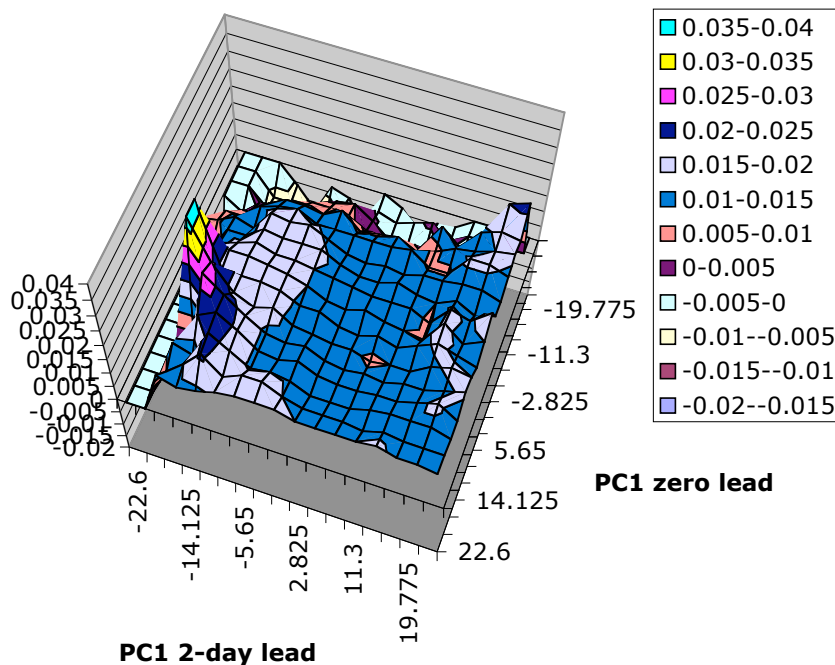


Figure 5.10: The difference between the April-May background ozone and June-July background ozone in HGA, as a function of PC1 with 2-day lead and PC1 with no lead.

The causes of this hemispheric springtime maximum remain somewhat controversial (Monks 2000; Vingarzan 2004). Other trace constituents show a maximum in springtime, including constituents with a wholly stratospheric origin and constituents with a wholly tropospheric origin. Thus, while troposphere-stratosphere exchange appears to play a role, other chemical mechanisms, such as wintertime buildup of pollutants followed by springtime photochemistry, must also be operating. Evaluation of global chemistry models by Wang et al. (1998) and Yienger et al. (1999) attribute the peak in rural areas to various combinations of transport from the stratosphere, tropospheric transport of ozone (with a long spring lifetime) from pollution sources, and photochemistry resulting from a wintertime buildup of NO_x. Closer to home, global model simulations show that the high springtime ozone over Bermuda is associated almost entirely with transport from North America, despite positive correlations with

stratospheric tracers (Li et al. 2002), while springtime tropospheric ozone over North America north of 40N above 5 km has a much stronger stratospheric source (Wang et al. 2003). It is likely that the Bermuda measurements and analyses are representative of conditions in the subtropical western Atlantic, the area of origin of air transported to Texas from the southeast in springtime. Given the longer lifetime of tropospheric ozone in the cool season, the potential contribution to springtime background ozone in Texas from Asian sources should also be considered.

DFW has a similar dependence on background ozone, but with some crucial differences (Fig. 5.11). First, the two-day lead plot is not shown here because the dependence on two-day lead PC1 is much weaker than at HGA. Apparently, DFW's closeness to continental anthropogenic sources reduces the need for several days of transport. Second, the area of high background ozone is broader, and the total variation of background ozone across the diagram is smaller, than in the corresponding HGA plot (Fig. 5.8). This means that DFW is less sensitive to the details of transport, making its late summer background ozone maximum less sharp than at HGA. Also, elevated background ozone levels are found in the vicinity of $PC1 = 0$ at zero and one-day leads, while at HGA the PC1 components needed to be negative before significantly elevated ozone was likely. This means that as the season progresses and PC1 becomes increasingly negative, DFW and other northern areas will see an increase of background ozone before HGA and more southern areas. This makes sense because winds from the east-southeast, corresponding to slightly negative PC1, would advect continental air to DFW but maritime air to HGA.

DFW Background Ozone

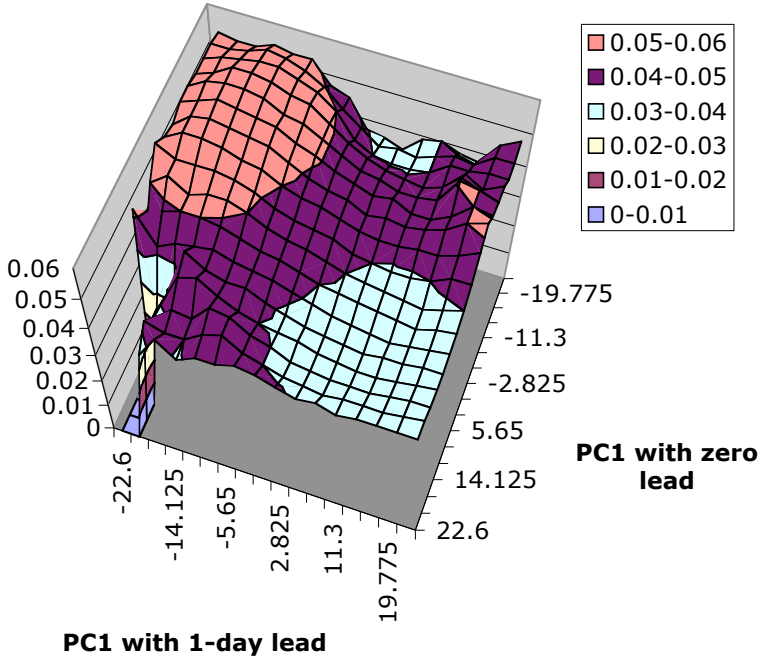


Figure 5.11: Background ozone in DFW as a function of PC1 with one-day lead and PC1 with zero lead.

6. Results

The key results of this research are as follows:

- (1) The intraseasonal variability in 8-h maximum ozone in eastern Texas is primarily associated with background ozone. Local contributions tend to be highest during the summer when background ozone reaches a local or global minimum.
- (2) The late spring peak in 8-h maximum ozone in eastern Texas is primarily associated with “tropospheric background” ozone. This ozone maximum has been observed at rural sites elsewhere, and is associated with variations in the lifetime of ozone, the concentrations of NO_x, and enhanced transport from the stratosphere.
- (3) The midsummer minimum in background ozone in eastern Texas leads to a minimum in 8-h maximum ozone that is strongest to the south and barely noticeable to the north. The primary cause of the summertime minimum is a decline in the tropospheric background ozone. Although the relatively clean southerly flow is weakening during this period, most air parcel paths remain maritime in nature.
- (4) As an easterly or northeasterly wind becomes more and more frequent later in the summer, background and total ozone in eastern Texas begin rising. This takes place first in northern regions of eastern Texas where southeasterly winds bring dirty air, then in more southern regions later in August as large-scale easterlies and northeasterlies develop. Winds are also less steady than in the middle of summer, so continental transport becomes increasingly frequent.
- (5) The peak 8-h ozone concentrations in eastern Texas occur at a time when the local contribution is still significant and the background ozone is increasing.

References

- Li, Q., D. J. Jacob, T. D. Fairlie, H. Liu, R. V. Martin, and R. M. Yantosca, 2002: Stratospheric versus pollution influences on ozone at Bermuda: Reconciling past analyses. *J. Geophys. Res.*, **107**, D22, 4611, doi:10.1029/2002JD002138.
- Monks, P. S., 2000: A review of the observations and origins of the spring ozone maximum. *Atmos. Env.*, **34**, 3545-3561.
- Vingarzan, R., 2004: A review of surface ozone background levels and trends. *Atmos. Env.*, **38**, 3431-3442.
- Wang, Y., D. J. Jacob, and J. A. Logan, 1998: Global simulation of tropospheric O₃-NO_x-hydrocarbon chemistry. 3. Origin of tropospheric ozone and effects of nonmethane hydrocarbons. *J. Geophys. Res.*, **103**, D9, 10 757-10 767.
- Wang, Y., C. Shim, N. Blake, D. Blake, Y. Choi, B. Ridley, J. Dibb, A. Wimmers, J. Moody, F. Flocke, A. Weinheimer, R. Talbot, and E. Atlas, 2003: Intercontinental transport of pollution manifested in the variability and seasonal trends of springtime O₃ at northern middle and high latitudes. *J. Geophys. Res.*, **108**, D21, 4683, doi:10.1029/2003JD003592.
- Yienger, J. J., A. A. Klonecki, H. Levy II, W. J. Moxim, and G. R. Carmichael, 1999: An evaluation of chemistry's role in the winter-spring ozone maximum found in the northern midlatitude free troposphere. *J. Geophys. Res.*, **104**, D3, 3655-3667.